

Guaranteed and computable error bounds for approximations constructed by an iterative decoupling of the Biot problem

Kundan Kumar*, Svetlana Kyas†, Jan Martin Nordbotten*, and Sergey Repin §

*Department of Mathematics, University of Bergen, Norway;

†Geothermal Energy and Geofluids, Institute of Geophysics, ETH Zürich, Switzerland

§ University of Jyväskylä, Finland; Steklov Inst. Math. of the RAS at St. Petersburg; Peter the Great Polytechnic University, St. Petersburg, Russia.

Abstract

The paper is concerned with guaranteed a posteriori error estimates for a class of evolutionary problems related to poroelastic media governed by the quasi-static linear Biot equations. The system is decoupled employing the fixed-stress split scheme, which leads to a semi-discrete system solved iteratively. The error bounds are derived by combining a posteriori estimates for contractive mappings with those of the functional type for elliptic partial differential equations. The estimates are applicable for any approximation in the admissible functional space and are independent of the discretization method. They are fully computable, do not contain mesh dependent constants, and provide reliable global estimates of the error measured in the energy norm. Moreover, they suggest efficient error indicators for the distribution of local errors, which can be used in adaptive procedures.

Keywords: Biot problem, fixed-stress split iterative scheme, a posteriori error estimates, contraction mappings.

1. Introduction

Problems defined in a poroelastic medium contribute to a wide range of application areas including simulation of oil reservoirs, prediction of the environmental changes, soil subsidence and liquefaction in the earthquake engineering, well stability, sand production, waste deposition, hydraulic fracturing, CO₂ sequestration, and understanding of the biological tissues in biomechanics. In recent years, mathematical modeling of poroelastic problems has become a highly important topic because it helps engineers to understand and predict complicated phenomena arising in such media as well as assists in preventing possible future financial calamities. However, numerical schemes designed for any of the existing models provide approximations that contain errors of different nature, which must be controlled. Therefore, a reliable quantitative analysis of poroelasticity problems requires efficient and computable error estimates that could be applied for various approximations and computation methods.

Mathematical modeling of poroelasticity is usually based on the Biot model that consists of the elasticity equation coupled with the equation describing the slow motion of the fluid. Computational errors in one part of the model may seriously affect the accuracy of the other one. Therefore, getting reliable and efficient a posteriori error estimates for coupled problems is, in general, a much more complicated task than for a single equation.

The Biot model is a system describing the flow and the displacement in a porous medium by momentum and mass conservation equations. Initially, it was derived at a macroscopic scale (with inertia effects negligible) in the works Terzaghi [1] and Biot [2]. The settlement of different types of soils was predicted in [1], which later was extended to the generalized theory of consolidation [2, 3]. A comprehensive discussion of the theory of poromechanics can be found in [4]. Thus, for modeling of the *solid displacement* \mathbf{u} and the *fluid pressure* p , we consider the system that governs the coupling of an *elastic isotropic porous medium* saturated with *slightly compressible viscous single-phase fluid*

$$\begin{aligned} -\operatorname{div}(\lambda(\operatorname{div}\mathbf{u})\mathbb{I} + 2\mu\boldsymbol{\varepsilon}(\mathbf{u}) - \alpha p\mathbb{I}) &= \mathbf{f} & \text{in } Q := \Omega \times (0, T), \\ \partial_t(\beta p + \alpha\operatorname{div}\mathbf{u}) - \operatorname{div}\mathbb{K}\nabla p &= g & \text{in } Q, \end{aligned} \quad (1.1)$$

where Q denotes a space-time cylinder (with bounded domain $\Omega \subset \mathbb{R}^d$, $d = \{2, 3\}$ having Lipschitz continuous boundary $\partial\Omega$ and given time-interval $(0, T)$, $0 < T < +\infty$), $\mathbf{f} \in H^1(0, T; [\mathbb{L}^2(\Omega)]^d)$ and $g \in L^2(0, T; L^2(\Omega))$ are the

body force and the volumetric fluid source, respectively¹. The first equation in (1.1) follows from the balance of linear momentum for the *total Cauchy stress tensor*

$$\boldsymbol{\sigma}_{\text{por}} := \boldsymbol{\sigma}(\mathbf{u}) - \alpha p \mathbb{I}$$

that accounts not only \mathbf{u} but also the pressure p scaled by the dimensionless Biot-Willis coefficient $\alpha > 0$. Linear elastic tensor is governed by Hooke's law

$$\boldsymbol{\sigma}(\mathbf{u}) := 2\mu \boldsymbol{\varepsilon}(\mathbf{u}) + \lambda \text{tr} \boldsymbol{\varepsilon}(\mathbf{u}) \mathbb{I} = 2\mu \boldsymbol{\varepsilon}(\mathbf{u}) + \lambda (\text{div} \mathbf{u}) \mathbb{I},$$

where $\boldsymbol{\varepsilon}(\mathbf{u}) := \frac{1}{2}(\nabla \mathbf{u} + (\nabla \mathbf{u})^T)$ is the *tensor of small strains*. Here, $\lambda, \mu > 0$ are the *Lamé constants* proportional to Young's modulus E and Poisson's ratio ν via relations $\mu = \frac{E}{2(1+\nu)}$ and $\lambda = \frac{E\nu}{(1+\nu)(1-2\nu)}$. The second equation is the fluid mass conservation (continuity) equation in Q . Here, β stands for the *storage coefficient* and \mathbb{K} is the *permeability tensor* assumed to be symmetric, uniformly bounded, anisotropic, and heterogeneous in space and constant in time, i.e.,

$$\lambda_{\mathbb{K}} |\boldsymbol{\tau}|^2 \leq \mathbb{K}(x) \boldsymbol{\tau} \cdot \boldsymbol{\tau} \leq \mu_{\mathbb{K}} |\boldsymbol{\tau}|^2, \quad \lambda_{\mathbb{K}}, \mu_{\mathbb{K}} > 0, \quad \text{for all } \boldsymbol{\tau} \in \mathbb{R}^d. \quad (1.2)$$

Let $\Sigma = \partial\Omega \times (0, T)$ be a lateral surface of Q , whereas $\Sigma_0 := \partial\Omega \times \{0\}$ and $\Sigma_T := \partial\Omega \times \{T\}$ define the bottom and the top parts of the mantel, such that $\partial Q = \Sigma \cup \Sigma_0 \cup \Sigma_T$. The initial conditions are assumed to be as follows:

$$p(x, 0) = p^\circ \in H^1(\Omega) \quad \text{and} \quad \mathbf{u}(x, 0) = \mathbf{u}^\circ \in [H^1(\Omega)]^d \quad \text{on } \Sigma_0. \quad (1.3)$$

We introduce the following partitions of the boundary: $\partial\Omega = \Sigma_D^p \cup \Sigma_N^p = \Sigma_D^{\mathbf{u}} \cup \Sigma_N^{\mathbf{u}}$, where Σ_D^p and $\Sigma_D^{\mathbf{u}}$ must have positive measures, i.e., $|\Sigma_D^p|, |\Sigma_D^{\mathbf{u}}| > 0$, with corresponding boundary conditions (BCs):

$$\begin{aligned} p &= p_D & \text{on } \Sigma_D^p, \\ -\mathbb{K} \nabla p \cdot \mathbf{n} &= z_N & \text{on } \Sigma_N^p, \\ \mathbf{u} &= \mathbf{u}_D & \text{on } \Sigma_D^{\mathbf{u}}, \\ \boldsymbol{\sigma}_{\text{por}} \cdot \mathbf{n} &= \mathbf{t}_N & \text{on } \Sigma_N^{\mathbf{u}}. \end{aligned} \quad (1.4)$$

For the fluid content $\beta p + \alpha \text{div} \mathbf{u}$, we prescribe the following initial condition

$$\eta(x, 0) := \beta p(x, 0) + \alpha \text{div} \mathbf{u}(x, 0) = \beta p^\circ + \alpha \text{div} \mathbf{u}^\circ,$$

where p° and \mathbf{u}° are defined in (1.3). To simplify the exposition, we consider only homogeneous BCs, i.e., $p_D, z_N = 0$ and $\mathbf{u}_D, \mathbf{t}_N = \mathbf{0}$ for the time being, even though all results are valid for more general assumptions.

The work [5] provides the results on existence, uniqueness, and regularity theory for (1.1)–(1.4) in the Hilbert space setting, whereas [6] extends the recent results to a wider class of diffusion problems in the poroelastic media with more general material deformation models. Corresponding a priori error estimates can be found in [7]. Considered system can be understood as the singular limit of the fully dynamic Biot-Allard problem (see the details in [8]), where the acceleration of the solid in the mechanics part of (1.1) is neglected.

As the Biot model is a coupled system of partial differential equations (PDEs), we have iterative as well as monolithic approaches used for solving the problem (see, e.g., [9]). For the first approach, the problem can be reformulated with a contractive operator, which naturally yields iteration methods for its solution (see [8]). On each step in the time, the flow problem is considered first. It is followed by solving the mechanics using already recovered pressure. The procedure is iterated until the desired convergence is reached. Different alteration of iterative cycles in flow and mechanics, i.e., single- [10] and multi-rate schemes [11, 12], can be considered. The second approach is fully coupled and considers the system with two unknowns simultaneously.

The iterative coupling offers several advantages over the monolithic method in the code design. In particular, in terms of availability of highly developed discretization methods (primal [13, 14, 15], mixed [7, 16, 17], Galerkin least-squares [18], finite volume (FV) [19], discontinuous Galerkin (dG) methods [20], high-order methods [21]

¹For convenience of the reader, we collected the definitions related to the functional spaces in Appendix

isogeometric analysis [22], as well as combinations of above-mentioned ones) and algebraic solvers (e.g., general Schur complement based preconditioners [23, 24, 25, 26, 27, 28, 29, 30], and the recently developed robust ones with respect to (w.r.t.) the model parameters [31, 32, 33, 34, 35]). In the fully-coupled methods, constructing efficient preconditioning techniques for the arising algebraic systems remains a matter of active ongoing scientific research (see, e.g., [36, 37, 30, 38, 39]).

The question of a posteriori error control for the poroelastic models has been already addressed using different techniques. Application of the residual-based error estimates to the coupled elliptic-parabolic problems can be traced back to works [40, 41]. Recently, similar error indicators were used in [42, 43, 44, 45, 46] for immiscible incompressible two- or multi-phase flows in porous media to address the questions of adaptive stopping criteria and mesh refinement. In [47], authors suggest an a posteriori error estimator based on the appropriate dual problem in space-time for a coupled consolidation problem involving large deformations. In [48, 49, 50, 51], adaptive space-time algorithms, relying on equilibrated fluxes technique, were applied to the Biot's consolidation model (formulated as a system with four unknowns). In this work, however, we turn to the functional error estimates (majorants and minorants), which are fully computable and provide guaranteed bounds of errors arising in the numerical approximations. The derivation of such estimates is based on functional arguments and variational formulation of the problem in question. Therefore, the method does not use specific properties of approximations (e.g., Galerkin orthogonality) and special properties of the exact solution (e.g., high regularity). The estimates do not contain mesh dependent constants and are valid for any approximation in the natural energy class. Moreover, the majorant also yields an efficient error indicator, that provides mesh adaptation.

Our main goal is to deduce efficient a posteriori error estimates for the approximation of the system (1.1) and verify them in application to the numerical problems. In [52], a posteriori error estimates of the functional type has been derived for the stationary Barenblatt–Biot model of porous media. This paper deals with more complicated Biot problem presented by an elliptic–parabolic system of partial differential equations. Our approach is based on the contraction property of the iterative method [53], which is rather general and not just restricted to fixed-stress scheme and functional type estimates of each equation in the Biot system (see, e.g., [54]). To the best knowledge of the authors, it is the first study targeting such a coupling between the elastic behavior of the medium and the fluid flow in a context of functional error estimates. The main result is presented in Theorem 3. Moreover, they not only serve as reliable estimates of the global error measured in the energy norm but also as an efficient indicator of the local error distribution over the computational domain (confirmed by majorant application to each of the decoupled problems in [55] and references therein). The latter property makes functional majorants advantageous in application to automated adaptive mesh generation algorithms.

The paper has the following structure: Section 2 is dedicated to the generalized formulation of the Biot system and its semi-discrete counterpart derived after applying the explicit Euler scheme in time. In Sections 3, we introduce an incremental approach, namely, fixed-stress split scheme, for discretizing considered coupled system. In particular, it justifies the optimal choice of parameters in the iterative scheme and proves that it is a contraction with an explicitly computable convergence rate. Sections 4 and 5 are dedicated to the derivation of auxiliary Lemmas used in the proof of Theorems 2 and 3 with the general estimates for the approximations generated by the fully decoupled iterative approach. Finally, Section 6 contains a collection of examples, which illustrates the application of derived error estimates to the Biot problem.

2. Variational formulation and discretization

We study approximations of the system (1.1), where $\tilde{\mathbf{V}} \equiv H^1(0, T; [H^1(\Omega)]^d)$ denotes the space for u (field of displacements) and $\tilde{W} \equiv H^1(0, T; H^1(\Omega))$ is the space for the variable p (pressure). The generalized setting of (1.1) reads: find a pair $(\mathbf{u}, p) \in \tilde{\mathbf{V}}_0 \times \tilde{W}_0$ such that

$$2\mu(\varepsilon(\mathbf{u}), \varepsilon(\mathbf{v}))_Q + \lambda(\operatorname{div}\mathbf{u}, \operatorname{div}\mathbf{v})_Q + \alpha(\nabla p, \mathbf{v})_Q = (\mathbf{f}, \mathbf{v})_Q, \quad \forall \mathbf{v} \in \tilde{\mathbf{V}}_0, \quad (2.1)$$

$$(\mathbf{K}\nabla p, \nabla w)_Q + (\partial_t(\beta p + \alpha \operatorname{div}\mathbf{u}), w)_Q = (g, w)_Q, \quad \forall w \in \tilde{W}_0, \quad (2.2)$$

where

$$\begin{aligned} \tilde{\mathbf{V}}_0 &:= \{v \in H^1(0, T; [H^1(\Omega)]^d) \mid \mathbf{v}(t)|_{\Sigma_D^v} = \mathbf{0} \text{ a.e. } t \in (0, T)\}, \\ \tilde{W}_0 &:= \{w \in H^1(0, T; H^1(\Omega)) \mid w(t)|_{\Sigma_D^p} = 0 \text{ a.e. } t \in (0, T)\}. \end{aligned}$$

The Biot system of type (2.1)–(2.2) was analyzed by several authors to establish existence, uniqueness, and regularity. The first theoretical results on the existence and uniqueness of a (weak) solution are presented in [56] for the case of $\beta = 0$. Further work in this direction can be found in [5, 57]. The well-posedness of the quasi-static Biot system is ensured under the above-mentioned assumptions. In fact, [58, 59] established contractive results in suitable norms for iterative coupling of (2.1)–(2.2). For an overview of the stability of existing iterative algorithms, we refer the reader to [60, 61].

The system (2.1)–(2.2) can be viewed as the two-field formulation of the poroelasticity problem. In numerical analysis, there are alternative approaches to treat such a system as *three- and four-field formulations*. In the case of the three-field model, an additional variable is introduced to represent the flux in the flow equations, whereas the four-field model considers stress as yet another unknown. Three-field formulation is rather flexible (since it allows different combinations of discretizations) and is accepted by the community as providing more physical approximations of the unknowns than in the two-field case. Recently, four-field formulation received increasing attention from the research community, where both equations were treated by mixed methods. The advantages of the latter representation are local conservation of mass and momentum balance and more accurate representation of fluxes and stresses. The choice of the formulation (from the above-mentioned list) is usually motivated by the considered application as well as the restriction on the computational resources. For instance, the mixed formulation of (2.2) does not only provide the flux that satisfies the local mass conservation property but also generates an effective approximation of this function, which is advantageous to functional type error control. It practically minimizes the majorant related to the pressure function (see (4.2)). The same method/principle works for the reconstruction of the stress field.

The system (2.1)–(2.2) is considered in the time-interval $[0, T]$ divided by N sub-intervals, such that it forms the corresponding set $\mathcal{T}_N = \cup_{n=1}^N I^n$, $I^n = (t^{n-1}, t^n)$. Let $\mathbf{u}^n(x) \in \mathbf{V}_0$ and $p^n(x) \in W_0$, where

$$\mathbf{V}_0 := \{\mathbf{v} \in \mathbf{V} \equiv [H^1(\Omega)]^d \mid \mathbf{v}|_{\Sigma_B} = 0\} \quad \text{and} \quad W_0 := \{w \in W \equiv H^1(\Omega) \mid w|_{\Sigma_D} = 0\}, \quad (2.3)$$

respectively, the spatial parts of the solution at $t = t^n$. Then, the semi-discrete approximation of (2.1)–(2.2) satisfies the system

$$\begin{aligned} (2\mu \boldsymbol{\varepsilon}(\mathbf{u}^n), \boldsymbol{\varepsilon}(\mathbf{v}))_\Omega + (\lambda \operatorname{div} \mathbf{u}^n, \operatorname{div} \mathbf{v})_\Omega + \alpha (\nabla p^n, \mathbf{v})_\Omega &= (\mathbf{f}^n, \mathbf{v})_\Omega, \quad \forall \mathbf{v} \in \mathbf{V}_0, \\ (\mathbb{K} \nabla p^n, \nabla w)_\Omega + \frac{1}{\tau^n} (\beta(p^n - p^{n-1}), w)_\Omega + \alpha \operatorname{div}(\mathbf{u}^n - \mathbf{u}^{n-1}), w)_\Omega &= (g^n, w)_\Omega, \quad \forall w \in W_0, \end{aligned}$$

where $\tau^n = t^n - t^{n-1}$. This system generates the following problem to be solved on each step of the time-incremental method: find the pair $(\mathbf{u}, p)^n \in \mathbf{V}_0 \times W_0$

$$(2\mu \boldsymbol{\varepsilon}(\mathbf{u}^n), \boldsymbol{\varepsilon}(\mathbf{v}))_\Omega + (\lambda \operatorname{div} \mathbf{u}^n, \operatorname{div} \mathbf{v})_\Omega + \alpha (\nabla p^n, \mathbf{v})_\Omega = (\mathbf{f}^n, \mathbf{v})_\Omega, \quad \forall \mathbf{v} \in \mathbf{V}_0, \quad (2.4)$$

$$(\mathbb{K}_{\tau^n} \nabla p^n, \nabla w)_\Omega + \beta (p^n, w)_\Omega + \alpha (\operatorname{div} \mathbf{u}^n, w)_\Omega = (\tilde{g}^n, w)_\Omega, \quad \forall w_0 \in W_0, \quad (2.5)$$

where $\mathbb{K}_{\tau^n} := \tau^n \mathbb{K}$, the right-hand side of (2.5) is defined as

$$\tilde{g}^n = \tau^n g^n + \beta p^{n-1} + \alpha \operatorname{div} \mathbf{u}^{n-1}, \quad (2.6)$$

and the pair $(\mathbf{u}, p)^{n-1} \in \mathbf{V}_0 \times W_0$ is given by the previous time step. The initial values are chosen as $(\mathbf{u}, p)^0 = (p^\circ, \mathbf{u}^\circ)$. Since from now on, we deal only with the semi-discrete counterpart of Biot problem, we omit the subscript Ω in the scalar product. Moreover, we always consider (2.4)–(2.5) on n th time step, which allows us to omit the superscript n for the rest of the paper and consider the system

$$(2\mu \boldsymbol{\varepsilon}(\mathbf{u}), \boldsymbol{\varepsilon}(\mathbf{v})) + (\lambda \operatorname{div} \mathbf{u}, \operatorname{div} \mathbf{v}) + \alpha (\nabla p, \mathbf{v}) = (\mathbf{f}, \mathbf{v}), \quad \forall \mathbf{v} \in \mathbf{V}_0, \quad (2.7)$$

$$(\mathbb{K}_\tau \nabla p, \nabla w) + \beta (p, w) + \alpha (\operatorname{div} \mathbf{u}, w) = (\tilde{g}, w), \quad \forall w \in W_0. \quad (2.8)$$

This work aims to derive a fully guaranteed a posteriori estimates of the error between the obtained approximations $(\tilde{\mathbf{u}}, \tilde{p}) \in \mathbf{V}_{0h} \times W_{0h}$, where \mathbf{V}_{0h} and W_{0h} are discretization spaces of conforming approximations of functional spaces \mathbf{V}_0 and W_0 , respectively, and the pair of the exact solutions (\mathbf{u}, p) of the Biot system, which is accumulated from the errors on all N time steps, i.e.,

$$e_{\mathbf{u}} := \mathbf{u} - \tilde{\mathbf{u}} \quad \text{and} \quad e_p := p - \tilde{p}.$$

On each time step, these errors are measured in terms of the combined norm

$$[[e_{\mathbf{u}}, e_p]] := \|e_{\mathbf{u}}\|_{\mathbf{u}}^2 + \|e_p\|_p^2. \quad (2.9)$$

In turn, each term of the error norm is defined as follows:

$$\|e_{\mathbf{u}}\|_{\mathbf{u}}^2 := \|\boldsymbol{\varepsilon}(e_{\mathbf{u}})\|_{2\mu}^2 + \|\operatorname{div}(e_{\mathbf{u}})\|_{\lambda}^2 \quad \text{and} \quad \|e_p\|_p^2 := \|\nabla e_p\|_{\mathbb{K}_\tau}^2 + \|e_p\|_{\beta}^2, \quad (2.10)$$

where $\|w\|_{\lambda}^2 := \int_{\Omega} \lambda w^2 dx$, $\|\boldsymbol{\varepsilon}(\mathbf{w})\|_{2\mu}^2 := \int_{\Omega} 2\mu \boldsymbol{\varepsilon}(\mathbf{w}) : \boldsymbol{\varepsilon}(\mathbf{w}) dx$, and $\|\mathbf{w}\|_{\mathbb{K}_\tau}^2 := \int_{\Omega} \mathbb{K}_\tau \mathbf{w} \cdot \mathbf{w} dx$ are L^2 -norms respectively weighted with 2μ , λ , and tensor \mathbb{K}_τ for any scalar- and vector-valued functions w and \mathbf{w} . The global bound of the errors $e_{\mathbf{u}}$ and e_p contains incremental contributions from each time-interval, i.e.,

$$\sum_{n=1, \dots, N} [[e_{\mathbf{u}}^{(n)}, e_p^{(n)}]] =: [[e_{\mathbf{u}}, e_p]] \leq \bar{\mathbf{M}}(\tilde{\mathbf{u}}, \tilde{p}) := \sum_{n=1, \dots, N} \bar{\mathbf{M}}^{(n)}(\tilde{\mathbf{u}}, \tilde{p}). \quad (2.11)$$

For the iterative approach, on each time-step I^n , the Biot system is decoupled into two sub-problems related to the linear elasticity and a single-phase flow problem. Then, an iterative procedure is applied to obtain the pair $(\mathbf{u}^i, p^i) = (\mathbf{u}, p)^i$. Next, each equation is discretized and solved, such that instead of $(\mathbf{u}, p)^i$ the pair $(\mathbf{u}, p)_h^i$, containing the approximation error of the numerical method, is used. In Section 4, we derive computable a posteriori estimates for this pair of approximate solution.

Functional $\bar{\mathbf{M}} := \bar{\mathbf{M}}^{(n)}$ (Theorem 3) is derived by combining the estimates derived for the contractive mapping [53] and the a posteriori error majorants for the elliptic problems (initially introduced [63, 64]). The validity of such estimates is based on the contraction property of specifically constructed linear combination of displacement and pressure $\frac{\alpha}{\gamma} \operatorname{div} \mathbf{u}^i - \frac{L}{\gamma} p^i$, $L, \gamma > 0$, (the so-called *volumetric mean stress*). The selection of the parameters L and γ is justified and explained in Section 3.

Remark 1. For the alternative monolithic approach, one solves (2.7)–(2.8) simultaneously for pressure and displacement, reconstructing the pair of approximations $(\tilde{\mathbf{u}}, \tilde{p}) = (\mathbf{u}_h, p_h) = (\mathbf{u}, p)_h$. For this case, the corresponding computable bound of the error between $(\tilde{\mathbf{u}}, \tilde{p})$ and the exact solution can be derived. Such a functional error bound is a combination of a posteriori error estimates for each of the unknowns in (2.7) and (2.8) (see, e.g., [65, 54] and references therein). For the detailed derivation, we refer the reader to [62].

Remark 2. We note that due to the Korn and Friedrichs' inequalities, both $\|e_{\mathbf{u}}\|^2$ and $\|e_{\mathbf{u}}\|_{\mathbf{u}}^2$ are estimated by $\|\boldsymbol{\varepsilon}(e_{\mathbf{u}})\|^2$. Moreover, the physical bound on the Lamé parameters is given as $d\lambda + 2\mu > 0$, in the most general case, allowing for the first parameter λ to be slightly negative for so-called auxetic materials. In this case, we use the fact that

$$\|e_{\mathbf{u}}\|_{\mathbf{u}}^2 := \|\boldsymbol{\varepsilon}(e_{\mathbf{u}})\|_{2\mu}^2 + \|\operatorname{div}(e_{\mathbf{u}})\|_{\lambda}^2 \stackrel{(6.5)}{\leq} (2\mu + d\lambda) \|\boldsymbol{\varepsilon}(e_{\mathbf{u}})\|^2$$

holds, and work with the positively-weighted norm $\|\boldsymbol{\varepsilon}(e_{\mathbf{u}})\|^2$. However, as auxetic materials are rare, the added complexity associated with allowing for such cases has been avoided in this paper. Consequently, the proofs below are based on the assumption of non-negative Lamé parameters.

3. Fixed-stress splitting scheme

Formal application of the iteration method to (2.7)–(2.8) yields the problem to be solved on the i th iteration step:

$$(\mathbb{K}_\tau \nabla p^i, \nabla w) + \beta (p^i, w) + \alpha (\operatorname{div} \mathbf{u}^{i-1}, w) = (\tilde{g}, w), \quad \forall w \in W_0, \quad (3.1)$$

$$(2\mu \boldsymbol{\varepsilon}(\mathbf{u}^i), \boldsymbol{\varepsilon}(\mathbf{v})) + (\lambda \operatorname{div} \mathbf{u}^i, \operatorname{div} \mathbf{v}) + \alpha (\nabla p^i, \mathbf{v}) = (\mathbf{f}, \mathbf{v}), \quad \forall \mathbf{v} \in \mathbf{V}_0, \quad (3.2)$$

where the flow equation (3.1) is solved for p^i , using \mathbf{u}^{i-1} , and the elasticity equation (3.2) is used to reconstruct \mathbf{u}^i using p^i recovered on the previous step. To obtain the initial data for the iteration procedure, we first set the pressure equal to the hydrostatic pressure, i.e., it follows from $\nabla p^0 = \rho_f g$ with $\rho_f > 0$ denoting the fluid phase density. Whereas \mathbf{u}^0 is reconstructed by (3.2) using p^0 . The iteration proposed in (3.1)–(3.2) is known as the *fixed strain*, and is only conditionally stable.

To stabilize the iteration scheme (3.1)–(3.2), we consider the ‘fixed-stress splitting approach’, which properties were initially studied in [61] and [58], respectively. This scheme operates with a special quantity: *volumetric mean total stress*

$$\eta^i = \frac{\alpha}{\gamma} \operatorname{div} \mathbf{u}^i - \frac{L}{\gamma} p^i \in W, \quad (3.3)$$

where γ and L are certain positive tuning parameters. These parameters are usually kept constant on each half-time step. The optimal choice of γ and L allows us to prove that this iteration scheme is a contraction in the L^2 -norm $\|\delta\eta^i\|^2$, where $\delta\eta^i := \eta^i - \eta^{i-1}$. Moreover, it accelerates the iteration procedure by reducing the number of iterations.

By adding $L(p^i - p^{i-1})$ into the right-hand side of (3.1), we rewrite the system (3.1)–(3.2) using the definition (3.3) as

$$(\mathbb{K}_\tau \nabla p^i, \nabla w) + (\beta + L)(p^i, w) = (\tilde{g} - \gamma \eta^{i-1}, w), \quad \forall w \in W_0, \quad (3.4)$$

$$(2\mu \boldsymbol{\varepsilon}(\mathbf{u}^i), \boldsymbol{\varepsilon}(\mathbf{v})) + (\lambda \operatorname{div} \mathbf{u}^i, \operatorname{div} \mathbf{v}) = (\mathbf{f}^i - \alpha \nabla p^i, \mathbf{v}), \quad \forall \mathbf{v} \in \mathbf{V}_0, \quad (3.5)$$

with complimented mixed BCs $p^i = 0$ on Σ_D^p and $\mathbb{K}_\tau \nabla p^i \cdot \mathbf{n} = 0$ on Σ_N^p as well as $\mathbf{u}^i = \mathbf{0}$ on Σ_D^u and $\boldsymbol{\sigma}_{\text{por}}^i \cdot \mathbf{n} = \mathbf{0}$ on Σ_N^u .

Let

$$\delta \nabla p^i := \nabla p^i - \nabla p^{i-1}, \quad \boldsymbol{\varepsilon}(\delta \mathbf{u}^i) := \boldsymbol{\varepsilon}(\mathbf{u}^i) - \boldsymbol{\varepsilon}(\mathbf{u}^{i-1}), \quad \delta \eta^i := \eta^i - \eta^{i-1}. \quad (3.6)$$

Theorem 1 establishes a contraction-type inequality for the norm $\|\delta\eta^i\|^2$.

Theorem 1 ([58, 59]). *If $\gamma = \frac{\alpha}{\sqrt{\lambda}}$ and $L \geq \frac{\alpha^2}{2\lambda}$, then (3.4)–(3.5) scheme is a contraction that satisfies the estimate*

$$\|\boldsymbol{\varepsilon}(\delta \mathbf{u}^i)\|_{2\mu}^2 + q \|\nabla \delta p^i\|_{\mathbb{K}_\tau}^2 + \|\delta \eta^i\|^2 \leq q^2 \|\delta \eta^{i-1}\|^2, \quad q = \frac{L}{\beta + L}, \quad (3.7)$$

where $\delta \nabla p^i$, $\boldsymbol{\varepsilon}(\delta \mathbf{u}^i)$, $\delta \eta^i$ are defined in (3.6).

Remark 3. *The estimates in Theorem 1, satisfying contraction estimate (3.7), also holds for Galerkin approximations $\{\delta\eta_h\}^i \in W_h$, where W_h is a discretization space of W . Moreover, in Appendix, we show that similar contraction theorem holds for sequence the $\{\delta(\eta - \eta_h)^i\} \in W_h$, where $\eta^i \in W$ is generated by the fixed-stress split iterative scheme defined in (3.4)–(3.5) and $\eta_h^i \in W_h$ is discretization of the latter sequence. Generally, it is important to note that all the theorems and lemmas below are formulated for a pair $(\mathbf{u}, p)^i \in \mathbf{V}_0 \times W_0$ that forms a contraction w.r.t. to $(\mathbf{u}, p)^{i-1} \in \mathbf{V}_0 \times W_0$ and its discrete approximation $(\mathbf{u}, p)_h^i \in \mathbf{V}_{0h} \times W_{0h}$ that forms a contraction relative to $(\mathbf{u}, p)_h^{i-1} \in \mathbf{V}_{0h} \times W_{0h}$.*

Remark 4. *There exist alternative ways to choose the tuning parameter L . In particular, the physically motivated choice $L_{\text{cl}} = \frac{\alpha^2}{\lambda + 2\mu/d}$ is considered in [61]. Whereas, [59] suggests $L_{\text{opt}} = \frac{\alpha^2}{2(\lambda + 2\mu/d)}$. The recent study [66] suggests the numerical evidence on the iteration counts w.r.t. the full range of the Lamé parameters for heterogeneous media. Numerical investigation of the optimality of these parameters and comparison with physically and mathematically motivated values from the literature was done in [67]. The authors demonstrated that their optimal value is not only dependent on the mechanical material parameters but on the boundary conditions and material parameters associated with the fluid flow problem.*

Remark 5. *The inequality (3.7) shows that the sequence $\{\delta\eta^i\}_{i \in \mathbb{N}}$ is generated by a contractive operator. Therefore, due to the Banach theorem, it tends to a certain fixed point. Moreover, since all the terms in the left-hand side of (3.7) are positive, in practice, $\{\delta\eta^i\}_{i \in \mathbb{N}}$ might converge with even better contraction rate than $q = \frac{L}{\beta + L}$.*

Corollary 1. *From Theorem 1, it follows that $\nabla \delta p^i$ and $\boldsymbol{\varepsilon}(\delta \mathbf{u}^i)$ in (3.6) are also converging sequences and satisfy*

$$\|\nabla \delta p^i\|_{\mathbb{K}_\tau}^2 \leq q \|\delta \eta^{i-1}\|^2 \quad \text{and} \quad \|\boldsymbol{\varepsilon}(\delta \mathbf{u}^i)\|_{2\mu}^2 \leq q^2 \|\delta \eta^{i-1}\|^2,$$

respectively.

Corollary 1 is used in the derivation of the error estimate for the term $\|e_p\|_p^2$. In particular, it yields the following result based on the estimates for the Banach contraction mappings (see [53, 54]).

Lemma 1 (Estimates for contractive mapping). *Let the assumptions of Theorem 1 hold. Then, we have the estimates*

$$\|\nabla(p - p^i)\|_{\mathbb{K}_\tau}^2 \leq \frac{q}{(1-q)^2} \|\delta\eta^{i-1}\|^2, \quad (3.8)$$

$$\|\varepsilon(\mathbf{u} - \mathbf{u}^i)\|_{2\mu} \leq \frac{q^2}{(1-q)^2} \|\delta\eta^{i-1}\|^2. \quad (3.9)$$

Proof: Consider

$$\begin{aligned} \|\nabla(p^{i+m} - p^i)\|_{\mathbb{K}_\tau} &\leq \|\nabla(p^{i+m} - p^{i+m-1})\|_{\mathbb{K}_\tau} + \dots + \|\nabla(p^{i+1} - p^i)\|_{\mathbb{K}_\tau} \\ &\leq q (\|\eta^{i+m-1} - \eta^{i+m-2}\| + \dots + \|\eta^i - \eta^{i-1}\|) \\ &\leq q (q^m + \dots + 1) \|\eta^i - \eta^{i-1}\|. \end{aligned}$$

By taking a limit $m \rightarrow \infty$ and noting that in this case $(q^m + q^{m-1} + \dots + 1) \rightarrow \frac{1}{1-q}$, we arrive at (3.8). The inequality (3.9) is proved by similar arguments. \square

If in Lemma 1, we consider iteration i and $i - m$, $i > m$ as two subsequent iterations, a more general version of estimates (3.8) and (3.9) can be formulated.

Lemma 2 (General estimates for contractive mapping). *Let the assumptions of Theorem 1 hold. Then, we have the estimates*

$$\|\nabla(p - p^i)\|_{\mathbb{K}_\tau}^2 \leq \min_{1 \leq m \leq i} \left\{ \frac{q^m}{(1-q^m)^2} \|\eta^i - \eta^{i-m}\|^2 \right\}, \quad (3.10)$$

$$\|\varepsilon(\mathbf{u} - \mathbf{u}^i)\|_{2\mu} \leq \min_{1 \leq m \leq i} \left\{ \frac{q^{2m}}{(1-q^m)^2} \|\eta^i - \eta^{i-m}\|^2 \right\}. \quad (3.11)$$

Proof: Proof follows along the lines of the proof of Lemma 1 with $m = 1, \dots, i$. \square

Remark 6. *Estimates in Lemma 2 improves the value of $\frac{q^m}{(1-q^m)^2}$ and $\frac{q^{2m}}{(1-q^m)^2}$ if q is close to 1. It might look contra intuitive, but the choice $m = i$ is not always most optimal. Simultaneously with the decrease of quotient with q , the term $\|\eta^i - \eta^0\|^2$ grows. Therefore, the choice of m must be made carefully. Computing majorant on each step of our iterative algorithm might be computationally expensive, therefore, in demanding applications, the choice of m must be done a priori. Alternatively, with several extra iterations made after reaching the desired convergence in p and \mathbf{u} , both $\frac{q^i}{(1-q^i)^2}$ with $q^i = q^m$ and $\|\eta^i - \eta^{i-m}\|^2$ will decrease, impacting the total values of the majorant.*

4. Estimates of errors generated by the discretization

Before deriving estimates of the approximation errors appearing in the contractive iterative scheme, we need to study discretization errors encompassed in (3.4)–(3.5) for the i th iteration. Henceforth, the pair $(\mathbf{u}, p)^i = (\mathbf{u}^i, p^i)$ is considered as the exact solution of (3.4)–(3.5), whereas $(\mathbf{u}, p)_h^i = (\mathbf{u}_h^i, p_h^i)$ denotes its approximation computed by a certain discretization method. We aim to derive computable and reliable estimates of the error measured in the terms $\|e_p^i\|_p^2$ and $\|e_{\mathbf{u}}^i\|_{\mathbf{u}}^2$.

Majorant of the error in the pressure term. For the first equation (3.4), Lemma 3 presents a computable upper bound of the difference

$$e_p^i := p^i - p_h^i$$

between the exact solution $p^i \in W_0$ and its approximation $p_h^i \in W_0$, measured in terms of the energy norm $\|e_p^i\|_p^2$.

Lemma 3. *For any $p_h^i \in W_0$, any auxiliary vector-valued function*

$$\mathbf{z}_h^i \in H_{\Sigma_N^p}(\Omega, \text{div}) := \{ \mathbf{z}_h^i \in [L(\Omega)]^d \mid \text{div} \mathbf{z}_h^i \in L2(\Omega), \mathbf{z}_h^i \cdot \mathbf{n} \in L2(\Sigma_N^p) \}, \quad (4.1)$$

and any parameter $\zeta \geq 0$, we have the following estimate

$$\|\nabla e_p^i\|_{\mathbb{K}_\tau}^2 + \|e_p^i\|_\beta^2 =: \|e_p^i\|_p^2 \leq \overline{M}_p^h(p_h^i, \mathbf{z}_h^i; \zeta),$$

where

$$\overline{M}_p^h(p_h^i, \mathbf{z}_h^i; \zeta) := (1 + \zeta) \|\mathbf{r}_d(p_h^i, \mathbf{z}_h^i)\|_{\mathbb{K}_\tau}^2 + (1 + \frac{1}{\zeta}) C_\Omega^p \left(\|\mathbf{r}_{\text{eq}}(p_h^i, \mathbf{z}_h^i)\|_\Omega^2 + \overline{M}_q^h((\mathbf{u}, p)_h^1) + \|\mathbf{z}_h^i \cdot \mathbf{n}\|_{\Sigma_N^p}^2 \right). \quad (4.2)$$

Here,

$$\mathbf{r}_d(p_h^i, \mathbf{z}_h^i) := \mathbf{z}_h^i - \mathbb{K}_\tau \nabla p_h^i, \quad \mathbf{r}_{\text{eq}}(p_h^i, \mathbf{z}_h^i) := \tilde{g} - \gamma \eta_h^{i-1} - (\beta + L) p_h^i + \text{div} \mathbf{z}_h^i,$$

where \tilde{g} is defined in (2.6), and

$$\overline{M}_q^h := \left(C_q \left(\frac{\alpha}{\gamma} \overline{M}_{p,L^2}^h + \frac{L}{\gamma} \overline{M}_{u,\text{div}}^h \right) + (C_q + 1) \|\eta^0 - \eta_h^0\| \right)^2,$$

where $\overline{M}_{p,L^2}^h(p_h^1, \mathbf{z}_h^1)$ and $\overline{M}_{u,\text{div}}^h((\mathbf{u}, p)_h^1, \boldsymbol{\tau}_h^1, \mathbf{z}_h^1)$ defined in Corollaries 2 and 3 dependent on explicitly given η^0 .
Constant

$$(C_\Omega^p)^2 := \frac{1}{(\beta+L)} \left(1 + (C_{\Sigma_N^p}^{\text{tr}})^2 \right) \quad (4.3)$$

is defined via the constant in the trace-type inequality

$$\|w\|_{\Sigma_N^p} \leq C_{\Sigma_N^p}^{\text{tr}} \|w\|_\Omega, \quad \forall w \in W_0, \quad (4.4)$$

and positive parameters of the Biot model β and L .

Proof: The majorant $\overline{M}_p(p_h^i, \mathbf{z}_h^i; \zeta)$ follows from [68, Section 2] and [54, Section 4.2–4.3], i.e., we consider (3.4) with subtracted from its left- and right-hand side bilinear form $(\mathbb{K}_\tau \nabla p_h^i, \nabla w) + (\beta + L)(p_h^i, w)$

$$(\mathbb{K}_\tau \nabla e_p^i, \nabla w) + (\beta + L)(e_p^i, w) = (\tilde{g} - \gamma \eta^{i-1} - (\beta + L) p_h^i, w) - (\mathbb{K}_\tau \nabla p_h^i, \nabla w).$$

Next, we set $w = e_p^i$ and introduce an auxiliary function $\mathbf{z}_h^i \in H_{\Sigma_N^p}(\Omega, \text{div})$ (cf. (4.1)) satisfying the identity $(\text{div} \mathbf{z}_h^i, \mathbf{w})_\Omega + (\mathbf{z}_h^i, \nabla \mathbf{w})_\Omega = (\mathbf{z}_h^i \cdot \mathbf{n}, \mathbf{w})_{\Sigma_N^p}$, such that

$$\begin{aligned} \|\nabla e_p^i\|_{\mathbb{K}_\tau}^2 + \|e_p^i\|_{\beta+L}^2 &= (\mathbf{z}_h^i - \mathbb{K}_\tau \nabla p_h^i, \nabla e_p^i) + (\tilde{g} - \gamma \eta^{i-1} - (\beta + L) p_h^i + \text{div} \mathbf{z}_h^i, e_p^i) - (\mathbf{z}_h^i \cdot \mathbf{n}, e_p^i)_{\Sigma_N^p} \\ &= (\mathbf{r}_d(p_h^i, \mathbf{z}_h^i), \nabla e_p^i) + (\tilde{\mathbf{r}}_{\text{eq}}(p_h^i, \mathbf{z}_h^i), e_p^i) - (\mathbf{z}_h^i \cdot \mathbf{n}, e_p^i)_{\Sigma_N^p}, \end{aligned} \quad (4.5)$$

where $\tilde{\mathbf{r}}_{\text{eq}}(p_h^i, \mathbf{z}_h^i) := \tilde{g} - \gamma \eta^{i-1} - (\beta + L) p_h^i + \text{div} \mathbf{z}_h^i$. Using the Hölder and Young inequalities, the first term on the right-hand side of (4.5) can be estimated as

$$(\mathbf{r}_d(p_h^i, \mathbf{z}_h^i), \nabla e_p^i) \leq \frac{1}{2} (1 + \zeta) \|\mathbf{r}_d(p_h^i, \mathbf{z}_h^i)\|_{1/\mathbb{K}_\tau}^2 + \frac{1}{2(1+\zeta)} \|\nabla e_p^i\|_{\mathbb{K}_\tau}^2. \quad (4.6)$$

The second term on the right-hand side of (4.5) is bounded analogously, i.e.,

$$(\tilde{\mathbf{r}}_{\text{eq}}(p_h^i, \mathbf{z}_h^i), e_p^i) - (\mathbf{z}_h^i \cdot \mathbf{n}, e_p^i)_{\Sigma_N^p} \leq \frac{1}{2} (1 + \frac{1}{\zeta}) (C_\Omega^p)^2 (\|\tilde{\mathbf{r}}_{\text{eq}}(p_h^i, \mathbf{z}_h^i)\|^2 + \|\mathbf{z}_h^i \cdot \mathbf{n}\|_{\Sigma_N^p}^2) + \frac{1}{2} \frac{\zeta}{1+\zeta} \|e_p^i\|_{\beta+L}^2, \quad (4.7)$$

where C_Ω^p (cf. (4.3)) is a constant in the inequality

$$\|w\|^2 + \|w\|_{\Sigma_N^p}^2 \leq (C_\Omega^p)^2 \|w\|_{\beta+L}^2, \quad \forall w \in W_0,$$

defined in (4.4). By summing up the results of (4.6) and (4.7), we obtain

$$\begin{aligned} \|\nabla e_p^i\|_{\mathbb{K}_\tau}^2 + \|e_p^i\|_\beta^2 &\leq \|\nabla e_p^i\|_{\mathbb{K}_\tau}^2 + \|e_p^i\|_{\beta+L}^2 \\ &\leq (1 + \zeta) \|\mathbf{r}_d(p_h^i, \mathbf{z}_h^i)\|_{1/\mathbb{K}_\tau}^2 + (1 + \frac{1}{\zeta}) (C_\Omega^p)^2 (\|\tilde{\mathbf{r}}_{\text{eq}}(p_h^i, \mathbf{z}_h^i)\|^2 + \|\mathbf{z}_h^i \cdot \mathbf{n}\|_{\Sigma_N^p}^2). \end{aligned} \quad (4.8)$$

At this point, the term $\|\tilde{\mathbf{r}}_{\text{eq}}(p_h^i, \mathbf{z}_h^i)\|^2$ is not fully computable in the usual sense of functional majorants since it is defined using η_{i-1} . However, it can be estimated by

$$\begin{aligned} \|\tilde{\mathbf{r}}_{\text{eq}}(p_h^i, \mathbf{z}_h^i)\|^2 &\leq \|\tilde{g} - \gamma \eta^{i-1} - (\beta + L)p_h^i + \text{div} \mathbf{z}_h^i\|^2 \\ &\leq 2\|\tilde{g} - \gamma \eta_h^{i-1} - (\beta + L)p_h^i + \text{div} \mathbf{z}_h^i\|^2 + 2\gamma^2 \|\eta^{i-1} - \eta_h^{i-1}\|^2 \\ &\leq 2\|\mathbf{r}_{\text{eq}}(p_h^i, \mathbf{z}_h^i)\|^2 + 2\gamma^2 \|\eta^{i-1} - \eta_h^{i-1}\|^2. \end{aligned} \quad (4.9)$$

Consider the norm $\|\eta^{i-1} - \eta_h^{i-1}\|$ (without the squares) and apply an approach similar to that was used in the proof of Lemma 1

$$\begin{aligned} \|\eta^i - \eta_h^i\| &\leq \sum_{k=1}^{i-1} \|\delta \eta^k - \delta \eta_h^k\| + \|\eta^0 - \eta_h^0\| \stackrel{\text{Theorem 4}}{\leq} (q^{i-1} + \dots + 1) \|\delta \eta^1 - \delta \eta_h^1\| + \|\eta^0 - \eta_h^0\| \\ &\leq \left(\sum_{k=1}^{i-1} q^k + 1 \right) \|\delta \eta^1 - \delta \eta_h^1\| + \|\eta^0 - \eta_h^0\| \\ &\leq \left(\sum_{k=1}^{i-1} q^k + 1 \right) (\|\eta^1 - \eta_h^1\| + \|\eta^0 - \eta_h^0\|) + \|\eta^0 - \eta_h^0\| \\ &\leq C_q \|\eta^1 - \eta_h^1\| + (C_q + 1) \|\eta^0 - \eta_h^0\|. \end{aligned}$$

Here, $\|\eta^0 - \eta_h^0\|$ is a computable term, whereas $\|\eta^1 - \eta_h^1\|^2$ is controlled by combination of majorants $\overline{\mathbf{M}}_{p, L^2}^h(p_h^1, \mathbf{z}_h^1)$ and $\overline{\mathbf{M}}_{u, \text{div}}^h((\mathbf{u}, p)_h^1, \boldsymbol{\tau}_h^1, \mathbf{z}_h^1)$ defined in Corollaries 2 and 3 containing computable $\eta^0 := \frac{\alpha}{\gamma} \text{div} \mathbf{u}^0 - \frac{L}{\gamma} p^0$, i.e.,

$$\|\eta^1 - \eta_h^1\| \leq \frac{\alpha}{\gamma} \|\text{div}(\mathbf{u}^1 - \mathbf{u}_h^1)\| + \frac{L}{\gamma} \|p^1 - p_h^1\| \leq \frac{\alpha}{\gamma} \left(\overline{\mathbf{M}}_{p, L^2}^h(p_h^1, \mathbf{z}_h^1; \zeta) \right)^{1/2} + \frac{L}{\gamma} \left(\overline{\mathbf{M}}_{u, \text{div}}^h((\mathbf{u}, p)_h^1, \boldsymbol{\tau}_h^1, \mathbf{z}_h^1) \right)^{1/2}. \quad (4.10)$$

This yields that

$$\|\eta^i - \eta_h^i\|^2 \leq \overline{\mathbf{M}}_q^h := \left(C_q \left(\frac{\alpha}{\gamma} \overline{\mathbf{M}}_{p, L^2}^h, 1/2 + \frac{L}{\gamma} \overline{\mathbf{M}}_{u, \text{div}}^h, 1/2 \right) + (C_q + 1) \|\eta^0 - \eta_h^0\| \right)^2 \quad (4.11)$$

The combination of (4.9) and (4.11) yields

$$\|\nabla e_p^i\|_{\mathbf{K}_\tau}^2 + \|e_p^i\|_\beta^2 \leq (1 + \zeta) \|\mathbf{r}_d(p_h^i, \mathbf{z}_h^i)\|_{1/\mathbf{K}_\tau}^2 + (1 + \frac{1}{\zeta}) (C_\Omega^p)^2 (2\|\mathbf{r}_{\text{eq}}(p_h^i, \mathbf{z}_h^i)\|^2 + \overline{\mathbf{M}}_q^h((\mathbf{u}, p)_h^1) + \|\mathbf{z}_h^i \cdot \mathbf{n}\|_{\Sigma_N^p}^2).$$

□

Remark 7. *The numerical reconstruction of the majorant involves several steps. They are motivated by the accuracy requirements imposed on the upper bound of the error. To generate guaranteed bounds with the realistic efficiency index $I_{\text{eff}}(\overline{\mathbf{M}}_p) := \frac{\overline{\mathbf{M}}_p}{\|p^i - p_h^i\|_p^2}$, we can reconstruct \mathbf{z}_h^i from ∇p_h^i (where p_h^i is approximated by the chosen discretization method recovering the exact solution of (3.4)). However, to obtain the sharpest estimate, functional $\overline{\mathbf{M}}_p$ must be optimized w.r.t. \mathbf{z}_h^i and ζ iteratively. This generates an auxiliary variational problem w.r.t. vector-valued function \mathbf{z}_h^i .*

Alternatively, one can consider the mixed formulation of (3.4) and reconstruct the pair (p_h^i, \mathbf{z}_h^i) simultaneously using one of the well-developed mixed methods [69, 70]. Then, both variables required for the reconstruction of $\overline{\mathbf{M}}_p$ are directly computable, and no additional post-processing (computational overhead) is required.

Majorant in Lemma 3 yields an estimate of the e_p^i measured in terms of L2-norm.

Corollary 2. *For any $p_h^i \in W_0$, any auxiliary functions and parameters defined in Lemma 3, the estimate*

$$\|e_p^i\|^2 \leq \overline{\mathbf{M}}_{p, L^2}^h(p_h^i, \mathbf{z}_h^i; \zeta) := \left(\tau \lambda_{\mathbf{K}}(C_{\Sigma_D^p}^F)^{-2} + \beta \right)^{-1} \overline{\mathbf{M}}_p^h(p_h^i, \mathbf{z}_h^i; \zeta) \quad (4.12)$$

holds, where $\overline{M}_p^h(p_h^i, z_h^i; \zeta)$ is defined in (4.2), $C_{\Sigma_D^p}^F$ is a constant in Friedrichs' inequality (cf. (6.2)), and λ_K is the minimum eigenvalue of the permeability tensor (cf. (1.2)).

Proof: By means of the Friedrichs' inequality and (1.2), we obtain

$$\|e_p^i\|_p^2 \geq \tau \lambda_K (C_{\Sigma_D^p}^F)^{-2} \|e_p^i\|^2 + \|e_p^i\|_\beta^2 \geq \left(\tau \lambda_K (C_{\Sigma_D^p}^F)^{-2} + \beta \right) \|e_p^i\|^2.$$

By combining (4.13) and (4.2), we arrive at (4.12). \square

Majorant of the error in the displacement term. Current section considers estimates for the error

$$e_{\mathbf{u}}^i := \mathbf{u}^i - \mathbf{u}_h^i \quad (4.13)$$

between the exact solution $\mathbf{u}^i \in \mathbf{V}_0$ and its respective approximation $\mathbf{u}_h^i \in \mathbf{V}_0$ measured in terms of the energy norm $\|\cdot\|_{\mathbf{u}}$ (cf. (2.10)). Since p_h^i is, in fact, used instead of p^i , the original problem (3.5) is replaced by

$$2\mu (\boldsymbol{\varepsilon}(\tilde{\mathbf{u}}^i), \boldsymbol{\varepsilon}(\mathbf{v})) + \lambda (\operatorname{div} \tilde{\mathbf{u}}^i, \operatorname{div} \mathbf{v}) = (\mathbf{f}^i - \alpha \nabla p_h^i, \mathbf{v}), \quad \forall \mathbf{v} \in \mathbf{V}_0, \quad (4.14)$$

with a perturbed right-hand side. Therefore, \mathbf{u}_h^i is an approximation of $\tilde{\mathbf{u}}^i$ instead of \mathbf{u}^i . In other words, $e_{\mathbf{u}}^i$ is composed of the error arising due to the original problem is replaced by (4.14), i.e., $\mathbf{u}^i - \tilde{\mathbf{u}}^i$, and the error $\tilde{\mathbf{u}}^i - \mathbf{u}_h^i$ arising because (4.14) is solved approximately. By means of the triangle inequality, $e_{\mathbf{u}}^i$ can be estimated by above-described errors as follows:

$$\|\boldsymbol{\varepsilon}(e_{\mathbf{u}}^i)\|_{2\mu}^2 + \|\operatorname{div}(e_{\mathbf{u}}^i)\|_\lambda^2 = \|e_{\mathbf{u}}^i\|_{\mathbf{u}}^2 \leq 2 \|\mathbf{u}^i - \tilde{\mathbf{u}}^i\|_{\mathbf{u}}^2 + 2 \|\tilde{\mathbf{u}}^i - \mathbf{u}_h^i\|_{\mathbf{u}}^2. \quad (4.15)$$

Here, $\|\tilde{\mathbf{u}}^i - \mathbf{u}_h^i\|_{\mathbf{u}}^2$ can be estimated by the functional majorant for a class of the elasticity problems (see Lemma 4), whereas $\|\mathbf{u}^i - \tilde{\mathbf{u}}^i\|_{\mathbf{u}}^2$ is controlled by the bound following from the difference of model problems (3.5) and (4.14) (see Lemma 5).

Lemma 4. For any $\mathbf{u}_h^i \in \mathbf{V}_0$ approximating $\tilde{\mathbf{u}}^i$ in (4.14), any auxiliary tensor-valued function

$$\boldsymbol{\tau}_h^i \in [\mathcal{T}_{\operatorname{Div}}(\Omega)]^{d \times d} := \left\{ \boldsymbol{\tau}_h^i \in [L^2(\Omega)]^{d \times d} \mid \operatorname{Div} \boldsymbol{\tau}_h^i \in [L^2(\Omega)]^d, \boldsymbol{\tau}_h^i \cdot \mathbf{n} \in L^2(\Sigma_N^{\mathbf{u}}) \right\},$$

and any parameter $\xi \geq 0$, we have the estimate

$$\begin{aligned} \|\boldsymbol{\varepsilon}(\tilde{\mathbf{u}}^i - \mathbf{u}_h^i)\|_{2\mu}^2 + \|\operatorname{div}(\tilde{\mathbf{u}}^i - \mathbf{u}_h^i)\|_\lambda^2 &= \|\tilde{\mathbf{u}}^i - \mathbf{u}_h^i\|_{\mathbf{u}}^2 \leq \overline{M}_{\tilde{\mathbf{u}}}((\mathbf{u}, p)_h^i, \boldsymbol{\tau}_h^i) \\ &:= (1 + \xi) \int_{\Omega} \mathbf{r}_d(p_h^i, \boldsymbol{\tau}_h^i) \, dx + (1 + \frac{1}{\xi}) C_{\Omega}^{\mathbf{u}} \left(\|\mathbf{r}_{\operatorname{eq}}(p_h^i, \boldsymbol{\tau}_h^i)\|_{\Omega}^2 + \|\boldsymbol{\tau}_h^i \cdot \mathbf{n}\|_{\Sigma_N^{\mathbf{u}}}^2 \right), \end{aligned} \quad (4.16)$$

where

$$\begin{aligned} \mathbf{r}_{\operatorname{eq}}(p_h^i, \boldsymbol{\tau}_h^i) &:= \mathbf{f}^i - \alpha \nabla p_h^i + \operatorname{Div} \boldsymbol{\tau}_h^i, \\ \mathbf{r}_{d,\mu,\lambda}(\mathbf{u}_h^i, \boldsymbol{\tau}_h^i) &:= 2\mu |\boldsymbol{\varepsilon}(\mathbf{u}_h^i)|^2 + \lambda |\operatorname{div} \mathbf{u}_h^i|^2 + \frac{1}{2\mu} (|\boldsymbol{\tau}_h^i|^2 - \frac{\lambda}{3\lambda+2\mu} |\operatorname{div} \boldsymbol{\tau}_h^i|^2) - 2\boldsymbol{\varepsilon}(\mathbf{u}_h^i) : \boldsymbol{\tau}_h^i, \end{aligned} \quad (4.17)$$

$\beta, \alpha, \mu, \lambda$ are characteristics of the Biot model, and

$$C_{\Omega}^{\mathbf{u}} := C^K (1 + C_{\Sigma_N^{\mathbf{u}}}^{\operatorname{tr}}) \quad (4.18)$$

is defined through the constants $C_{\Sigma_N^{\mathbf{u}}}^{\operatorname{tr}}$ and C^K in trace-type and the Korn first inequalities

$$\|\mathbf{w}\|_{\Sigma_N^{\mathbf{u}}} \leq C_{\Sigma_N^{\mathbf{u}}}^{\operatorname{tr}} \|\mathbf{w}\|_{[H^1(\Omega)]^d} \quad \text{and} \quad \|\mathbf{w}\|_{[H^1(\Omega)]^d} \leq C^K \|\boldsymbol{\varepsilon}(\mathbf{w})\|_{[L^2(\Omega)]^{d \times d}} \quad \forall \mathbf{w} \in \mathbf{V}_0, \quad (4.19)$$

respectively.

Proof: For the simplicity of exposition, let us assume the following representation of the elasticity tensor

$$\mathbb{L} \boldsymbol{\varepsilon}(\mathbf{u}) := 2\mu \boldsymbol{\varepsilon}(\mathbf{u}) + \lambda \operatorname{div}(\mathbf{u}). \quad (4.20)$$

Then, the derivation of an a posteriori error estimate for the problem

$$(\mathbb{L}\varepsilon(\tilde{\mathbf{u}}^i), \varepsilon(\mathbf{v})) = (\mathbf{f}^i - \alpha \nabla p_h^i, \mathbf{v}), \quad \forall \mathbf{v} \in \mathbf{V}_0, \quad (4.21)$$

follows the lines presented in [54, Section 5.2]. In particular, considering an approximation $\mathbf{u}_h^i \in \mathbf{V}_0$, we subtract bilinear form $(\mathbb{L}\varepsilon(\mathbf{u}_h^i), \varepsilon(\mathbf{v}))$ from the left- and right-hand side of (4.21) and set $\mathbf{v} = \tilde{\mathbf{u}}^i - \mathbf{u}_h^i$ to obtain

$$(\mathbb{L}\varepsilon(\tilde{\mathbf{u}}^i - \mathbf{u}_h^i), \varepsilon(\tilde{\mathbf{u}}^i - \mathbf{u}_h^i)) = (\mathbf{f}^i - \alpha \nabla p_h^i, \mathbf{v}) - (\mathbb{L}\varepsilon(\mathbf{u}_h^i), \varepsilon(\tilde{\mathbf{u}}^i - \mathbf{u}_h^i)). \quad (4.22)$$

Next, we set $\mathbf{v} = \tilde{\mathbf{u}}^i - \mathbf{u}_h^i$ and add the divergence of the tensor-valued function $\boldsymbol{\tau}_h^i \in [\mathcal{T}_{\text{Div}}(\Omega)]^{d \times d}$, i.e.,

$$(\text{Div} \boldsymbol{\tau}_h^i, \mathbf{v}) + (\boldsymbol{\tau}_h^i, \varepsilon(\mathbf{v})) = (\boldsymbol{\tau}_h^i \cdot \mathbf{n}, \mathbf{v})_{\Sigma_N^u}, \quad \forall \mathbf{v} \in \mathbf{V}_0, \quad (4.23)$$

into the left- and right-hand side of (4.22), which results in the identity

$$(\mathbb{L}\varepsilon(\tilde{\mathbf{u}}^i - \mathbf{u}_h^i), \varepsilon(\tilde{\mathbf{u}}^i - \mathbf{u}_h^i)) = (\mathbf{r}_{\text{d,L}}(\mathbf{u}_h^i, \boldsymbol{\tau}_h^i), \varepsilon(\tilde{\mathbf{u}}^i - \mathbf{u}_h^i)) + (\mathbf{r}_{\text{eq}}(p_h^i, \boldsymbol{\tau}_h^i), \tilde{\mathbf{u}}^i - \mathbf{u}_h^i) - (\boldsymbol{\tau}_h^i \cdot \mathbf{n}, \tilde{\mathbf{u}}^i - \mathbf{u}_h^i)_{\Sigma_N^u}, \quad (4.24)$$

where

$$\mathbf{r}_{\text{d,L}}(\mathbf{u}_h^i, \boldsymbol{\tau}_h^i) := \boldsymbol{\tau}_h^i - \mathbb{L}\varepsilon(\mathbf{u}_h^i)$$

and $\mathbf{r}_{\text{eq}}(p_h^i, \boldsymbol{\tau}_h^i)$ is defined (4.17). By means of the Hölder and Young inequalities, the first term on the right-hand side of (4.22) can be estimated as

$$(\mathbf{r}_{\text{d,L}}(\mathbf{u}_h^i, \boldsymbol{\tau}_h^i), \varepsilon(\tilde{\mathbf{u}}^i - \mathbf{u}_h^i)) \leq \|\mathbf{r}_{\text{d,L}}(\mathbf{u}_h^i, \boldsymbol{\tau}_h^i)\|_{\mathbb{L}^{-1}} \|\varepsilon(\tilde{\mathbf{u}}^i - \mathbf{u}_h^i)\|_{\mathbb{L}} \leq \frac{\alpha_1}{2} \|\mathbf{r}_{\text{d}}(\mathbf{u}_h^i, \boldsymbol{\tau}_h^i)\|_{\mathbb{L}^{-1}}^2 + \frac{1}{2\alpha_1} \|\varepsilon(\tilde{\mathbf{u}}^i - \mathbf{u}_h^i)\|_{\mathbb{L}}^2$$

The second and the third terms are combined and estimated as follows

$$(\mathbf{r}_{\text{eq}}(p_h^i, \boldsymbol{\tau}_h^i), \tilde{\mathbf{u}}^i - \mathbf{u}_h^i) - (\boldsymbol{\tau}_h^i \cdot \mathbf{n}, \tilde{\mathbf{u}}^i - \mathbf{u}_h^i)_{\Sigma_N^u} \leq \frac{\alpha_2}{2} (C_\Omega^u)^2 (\|\mathbf{r}_{\text{eq}}(p_h^i, \boldsymbol{\tau}_h^i)\|^2 + \|\boldsymbol{\tau}_h^i \cdot \mathbf{n}\|_{\Sigma_N^u}^2) + \frac{1}{2\alpha_2} \|\varepsilon(\tilde{\mathbf{u}}^i - \mathbf{u}_h^i)\|_{\mathbb{L}}^2$$

where C_Ω^u (cf. (4.18)) is a constant in

$$\|\tilde{\mathbf{u}}^i - \mathbf{u}_h^i\|^2 + \|\tilde{\mathbf{u}}^i - \mathbf{u}_h^i\|_{\Sigma_N^u}^2 \leq (C_\Omega^u)^2 \|\varepsilon(\tilde{\mathbf{u}}^i - \mathbf{u}_h^i)\|_{\mathbb{L}}^2$$

defined through constants C^K and $C_{\Sigma_N^u}^{\text{tr}}$ in the Korn and trace inequalities defined in (6.4) and (6.3), respectively.

By choosing parameters $\alpha_1 = (\xi + 1)$, $\alpha_2 = (1 + \frac{1}{\xi})$, where $\xi > 0$, we arrive at

$$\|\varepsilon(\tilde{\mathbf{u}}^i - \mathbf{u}_h^i)\|_{\mathbb{L}} \leq (1 + \xi) \|\mathbf{r}_{\text{d,L}}(\mathbf{u}_h^i, \boldsymbol{\tau}_h^i)\|_{\mathbb{L}^{-1}} + (1 + \frac{1}{\xi}) (C_\Omega^u)^2 (\|\mathbf{r}_{\text{eq}}(p_h^i, \boldsymbol{\tau}_h^i)\|^2 + \|\boldsymbol{\tau}_h^i \cdot \mathbf{n}\|_{\Sigma_N^u}^2). \quad (4.25)$$

Consider now (4.20) and the representation of tensor $\mathbb{L}^{-1}\boldsymbol{\tau}_h^i$ through Lamé parameters, i.e.,

$$\mathbb{L}^{-1}\boldsymbol{\tau}_h^i := \frac{1}{2\mu} (\boldsymbol{\tau}_h^i - \frac{\lambda}{3\lambda+2\mu} \text{div} \boldsymbol{\tau}_h^i \mathbb{I}).$$

Then, the first term on the right-hand side of (4.25) can be rewritten as

$$\begin{aligned} \mathbb{L}^{-1}\mathbf{r}_{\text{d,L}}(\mathbf{u}_h^i, \boldsymbol{\tau}_h^i) : \mathbf{r}_{\text{d,L}}(\mathbf{u}_h^i, \boldsymbol{\tau}_h^i) &= (\mathbb{L}^{-1}\boldsymbol{\tau}_h^i - \varepsilon(\mathbf{u}_h^i)) : (\boldsymbol{\tau}_h^i - \mathbb{L}\varepsilon(\mathbf{u}_h^i)) \\ &= 2\mu |\varepsilon(\mathbf{u}_h^i)|^2 + \lambda |\text{div} \mathbf{u}_h^i|^2 + \frac{1}{2\mu} (|\boldsymbol{\tau}_h^i|^2 - \frac{\lambda}{3\lambda+2\mu} |\text{div} \boldsymbol{\tau}_h^i|^2) - 2\varepsilon(\mathbf{u}_h^i) : \boldsymbol{\tau}_h^i =: \mathbf{r}_{\text{d},\mu,\lambda}. \end{aligned} \quad (4.26)$$

Taking the latter into account, we arrive at the alternative estimate

$$\begin{aligned} \|\varepsilon(\tilde{\mathbf{u}}^i - \mathbf{u}_h^i)\|_{2\mu}^2 + \|\text{div}(\tilde{\mathbf{u}}^i - \mathbf{u}_h^i)\|_{\lambda}^2 \\ \leq (1 + \xi) \int_{\Omega} \mathbf{r}_{\text{d},\mu,\lambda}(\mathbf{u}_h^i, \boldsymbol{\tau}_h^i) \, dx + (1 + \frac{1}{\xi}) (C_\Omega^u)^2 (\|\mathbf{r}_{\text{eq}}(p_h^i, \boldsymbol{\tau}_h^i)\|^2 + \|\boldsymbol{\tau}_h^i \cdot \mathbf{n}\|_{\Sigma_N^u}^2), \end{aligned} \quad (4.27)$$

where $\mathbf{r}_{\text{d},\mu,\lambda}(\mathbf{u}_h^i, \boldsymbol{\tau}_h^i)$ is defined in (4.26) and $\boldsymbol{\tau}_h^i = \boldsymbol{\tau}_h^i$ is an auxiliary stress approximating function reconstructed in the correspondence with \mathbf{u}_h^i . \square

Remark 8. We note the choice of the auxiliary tensor-function providing the optimal values of the error estimate is $\boldsymbol{\tau}_h^* := \mathbb{L}\boldsymbol{\varepsilon}(\tilde{\mathbf{u}}^i) := 2\mu\boldsymbol{\varepsilon}(\tilde{\mathbf{u}}^i) + \lambda\operatorname{div}(\tilde{\mathbf{u}}^i)\mathbb{I}$. In this case, we can show that the equilibration residual $\mathbf{r}_{\text{eq}}(p_h^i, \boldsymbol{\tau}_h^i)$ vanishes, and the dual one provides the exact representation of the error.

Lemma 5 proceeds with estimation of $e_{\mathbf{u}}^i$ (cf. (4.13)), accounting for the error arising if (3.5) is replaced by (4.14).

Lemma 5. For any $p_h^i \in W_0$, any $\mathbf{u}_h^i \in \mathbf{V}_0$ approximating $\tilde{\mathbf{u}}^i$ in (4.14), and any $\mathbf{z}_h^i \in H_{\Sigma_N^p}(\Omega, \operatorname{div})$ and $\boldsymbol{\tau}_h^i \in [\mathcal{T}_{\operatorname{Div}}(\Omega)]^{d \times d}$, the estimate

$$\|e_{\mathbf{u}}^i\|_{\mathbf{u}}^2 \leq \overline{M}_u^h((\mathbf{u}, p)_h^i, (\boldsymbol{\tau}, \mathbf{z})_h^i) := \frac{2\lambda\eta^2\alpha^2}{2\chi\lambda-1} \overline{M}_{p, L^2}^h(p_h^i, \mathbf{z}_h^i) + 2\overline{M}_{\tilde{\mathbf{u}}}((\mathbf{u}, p)_h^i, \boldsymbol{\tau}_h^i) \quad (4.28)$$

holds, where $\zeta \geq 0$ and $\chi \in [\frac{1}{2\lambda}, +\infty)$. Here, \overline{M}_{p, L^2} and $\overline{M}_{\tilde{\mathbf{u}}}$ are defined in (4.12) and (4.16), respectively, and α and λ are characteristics of the Biot model.

Proof: As it was noted in (4.15), the error is two-folded and composed from $\|\mathbf{u}^i - \tilde{\mathbf{u}}^i\|_{\mathbf{u}}^2$ and $\|\tilde{\mathbf{u}}^i - \mathbf{u}_h^i\|_{\mathbf{u}}^2$, where the second term is controlled by (4.16) in Lemma 4. The estimate of the first term is derived by considering the difference of (3.5) and (4.14), i.e.,

$$2\mu(\boldsymbol{\varepsilon}(\mathbf{u}^i - \tilde{\mathbf{u}}^i), \boldsymbol{\varepsilon}(\mathbf{v})) + \lambda(\operatorname{div}(\mathbf{u}^i - \tilde{\mathbf{u}}^i), \operatorname{div}\mathbf{v}) = -\alpha(p^i - p_h^i, \operatorname{div}\mathbf{v}).$$

By choosing $\mathbf{v} = \mathbf{u}^i - \tilde{\mathbf{u}}^i$, we obtain the identity

$$\|\boldsymbol{\varepsilon}(\mathbf{u}^i - \tilde{\mathbf{u}}^i)\|_{2\mu}^2 + \|\operatorname{div}(\mathbf{u}^i - \tilde{\mathbf{u}}^i)\|_{\lambda}^2 = -\alpha(p^i - p_h^i, \operatorname{div}(\mathbf{u}^i - \tilde{\mathbf{u}}^i)).$$

The latter one can be estimated from above by the Cauchy inequality, which yields

$$\|\boldsymbol{\varepsilon}(e_{\mathbf{u}}^i)\|_{2\mu}^2 + \|\operatorname{div}(e_{\mathbf{u}}^i)\|_{\lambda}^2 \leq \alpha\|e_p^i\| \|\operatorname{div}(e_{\mathbf{u}}^i)\|.$$

By using the Young inequality with $\chi \geq \frac{1}{2\lambda}$, we arrive at

$$\|\boldsymbol{\varepsilon}(\mathbf{u}^i - \tilde{\mathbf{u}}^i)\|_{2\mu}^2 + (\lambda - \frac{1}{2\chi}) \|\operatorname{div}(\mathbf{u}^i - \tilde{\mathbf{u}}^i)\|_{\lambda}^2 \leq \frac{\chi}{2}\alpha^2 \|p^i - p_h^i\|^2. \quad (4.29)$$

According to Lemma 2, the linear combination in (4.29) can be estimated as

$$\|\boldsymbol{\varepsilon}(\mathbf{u}^i - \tilde{\mathbf{u}}^i)\|_{2\mu}^2 + (\lambda - \frac{1}{2\chi}) \|\operatorname{div}(\mathbf{u}^i - \tilde{\mathbf{u}}^i)\|_{\lambda}^2 \leq \frac{\chi\alpha^2}{2} \overline{M}_{p, L^2}(p_h^i).$$

By using

$$\|\boldsymbol{\varepsilon}(\mathbf{u}^i - \tilde{\mathbf{u}}^i)\|_{2\mu}^2 + \|\operatorname{div}(\mathbf{u}^i - \tilde{\mathbf{u}}^i)\|_{\lambda}^2 \leq \frac{2\chi\lambda}{2\chi\lambda-1} \left(\|\boldsymbol{\varepsilon}(\mathbf{u}^i - \tilde{\mathbf{u}}^i)\|_{2\mu}^2 + (\lambda - \frac{1}{2\chi}) \|\operatorname{div}(\mathbf{u}^i - \tilde{\mathbf{u}}^i)\|_{\lambda}^2 \right),$$

we obtain

$$\|\mathbf{u}^i - \tilde{\mathbf{u}}^i\|_{\mathbf{u}}^2 \leq \frac{\lambda\chi^2\alpha^2}{2\chi\lambda-1} \overline{M}_{p, L^2}(p_h^i).$$

Combining (4.16) and (4.30), we arrive at

$$\|\boldsymbol{\varepsilon}(e_{\mathbf{u}}^i)\|_{2\mu}^2 + \|\operatorname{div}(e_{\mathbf{u}}^i)\|_{\lambda}^2 \leq \frac{2\lambda\chi^2\alpha^2}{2\chi\lambda-1} \overline{M}_{p, L^2}(p_h^i) + 2\overline{M}_{\tilde{\mathbf{u}}}(\mathbf{u}_h^i, p_h^i). \quad (4.30)$$

□

In addition to (4.16), we can obtain the estimate for the error measured in terms of $\|\operatorname{div} \cdot\|$ -norm.

Corollary 3. For any $p_h^i \in W_0$, any $\mathbf{u}_h^i \in \mathbf{V}_0$ approximating $\tilde{\mathbf{u}}^i$ in (4.14), as well as any parameters and function defined in Lemma 5, we have

$$\|\operatorname{div}(e_{\mathbf{u}}^i)\|_{\lambda}^2 \leq \overline{M}_{u, \operatorname{div}}^h((\mathbf{u}, p)_h^i, \boldsymbol{\tau}_h^i, \mathbf{z}_h^i) := \frac{1}{(2\mu d + \lambda)} \left(\frac{2\lambda\eta^2\alpha^2}{2\eta\lambda-1} \overline{M}_{p, L^2}(p_h^i, \mathbf{z}_h^i) + \overline{M}_{\tilde{\mathbf{u}}}((\mathbf{u}, p)_h^i, \boldsymbol{\tau}_h^i) \right), \quad (4.31)$$

where $\overline{M}_p(p_h^i, \mathbf{z}_h^i)$ and $\overline{M}_{\tilde{u}}((\mathbf{u}, p)_h^i, \boldsymbol{\tau}_h^i)$ are defined in (4.12) and (4.16) for any $\mathbf{z}_h^i \in H_{\Sigma_N^p}(\Omega, \text{div})$ and $\boldsymbol{\tau}_h^i \in [\mathcal{T}_{\text{Div}}(\Omega)]^{d \times d}$, respectively, and μ is characteristic of the Biot model.

Proof: By using inequality (6.5) and substituting it in (4.16), we arrive at

$$(2\mu d + \lambda) \|\text{div}(e_{\mathbf{u}}^i)\|^2 \leq \overline{M}_{u, \text{div}}(p_h^i, \mathbf{z}_h^i; \zeta) = \frac{2\lambda\eta^2\alpha^2}{2\eta\lambda-1} \overline{M}_{p, L^2}(p_h^i) + 2\overline{M}_{\tilde{u}}((\mathbf{u}, p)_h^i, \boldsymbol{\tau}_h^i).$$

□

5. Estimates of errors generated by the iteration method

Next, we consider guaranteed bounds of errors arising in the process of contractive iterations (3.4)–(3.5) applied to the system (2.7)–(2.8).

Error estimates for pressure term. First, we prove the following result for the error in the flow equation, which can be done in two different ways. For Lemma 6, we consider functions $p_h^i, p_h^{i-1} \in W_0$ as approximations of two consequent pressures associated with the iterations i and $i-1$, whereas $\mathbf{u}_h^i, \mathbf{u}_h^{i-1} \in \mathbf{V}_0$ are approximations of \tilde{u}^i and $\tilde{u}^{i-1} \in \mathbf{V}_0$ in (4.14), respectively. From now on, when we refer to both dual variables \mathbf{z}_h^i and $\boldsymbol{\tau}_h^i$ corresponding to the i th iteration step, we refer to them as a pair $(\boldsymbol{\tau}, \mathbf{z})_h^i$.

Lemma 6. For $p^i, p^{i-1} \in W_0$ approximating $p \in W_0$ in (2.8), the estimate of the error incorporated in the pressure term on the i th iteration step has the following form

$$\begin{aligned} \|p - p^i\|_p^2 &\leq \overline{M}_p^i((\mathbf{u}, p)_h^{i-1}, (\boldsymbol{\tau}, \mathbf{z})_h^{i-1}, (\mathbf{u}, p)_h^i, (\boldsymbol{\tau}, \mathbf{z})_h^i) := \frac{3q}{1-q^2} \left(\frac{(C_{\Sigma_D^p}^F)^2 \beta}{\lambda_{\mathbb{K}} \tau} + 1 \right) \left(\|\eta_h^i - \eta_h^{i-1}\|^2 \right. \\ &\quad \left. + \frac{\lambda}{2} (\overline{M}_{u, \text{div}}^h((\mathbf{u}, p)_h^i, (\boldsymbol{\tau}, \mathbf{z})_h^i) + \overline{M}_{u, \text{div}}^h((\mathbf{u}, p)_h^{i-1}, (\boldsymbol{\tau}, \mathbf{z})_h^{i-1})) \right. \\ &\quad \left. + \frac{L}{4} (\overline{M}_{p, L^2}^h(p_h^i, \mathbf{z}_h^i) + \overline{M}_{p, L^2}^h(p_h^{i-1}, \mathbf{z}_h^{i-1})) \right), \end{aligned} \quad (5.1)$$

where $\overline{M}_{u, \text{div}}^h$ and \overline{M}_{p, L^2}^h are defined in Corollaries 2 and 3 with $\boldsymbol{\tau}_h^i \in [\mathcal{T}_{\text{Div}}(\Omega)]^{d \times d}$ and $\mathbf{z}_h^i \in H_{\Sigma_N^p}(\Omega, \text{div})$, respectively, $q = \frac{L}{\beta+L}$, and

$$\eta_h^i = \frac{\alpha}{\gamma} \text{div} \mathbf{u}_h^i - \frac{L}{\gamma} p_h^i, \quad L \geq \frac{\alpha^2}{2\lambda}, \quad \forall p_h^i \in W_0, \mathbf{u}_h^i \in \mathbf{V}_0.$$

Parameters $\alpha, \beta, \lambda, \mu_f, C_{\Sigma_D^p}^F, \lambda_{\mathbb{K}}$, and τ are characteristics of the semi-discrete Biot model (3.2)–(3.1).

Proof: We begin by noting that for the error $p - p^i$ caused by the iterative scheme

$$\|p - p^i\|_p^2 = \|p - p^i\|_{\beta}^2 + \|\nabla(p - p^i)\|_{\mathbb{K}\tau}^2 \stackrel{(6.2)}{\leq} \left(\frac{(C_{\Sigma_D^p}^F)^2 \beta}{\lambda_{\mathbb{K}} \tau} + 1 \right) \|\nabla(p - p^i)\|_{\mathbb{K}\tau}^2. \quad (5.2)$$

The estimate of $\|\nabla(p - p^i)\|_{\mathbb{K}\tau}^2$ follows from (3.8). To proceed forward, we need to estimate the right-hand side of (3.8), namely $\|\eta^i - \eta^{i-1}\|^2$. By adding and extracting the discretized approximations η_h^{i-1} and η_h^i , we obtain

$$\|\eta^i - \eta^{i-1}\|^2 \leq 3 (\|\eta_h^i - \eta_h^{i-1}\|^2 + \|\eta^i - \eta_h^i\|^2 + \|\eta^{i-1} - \eta_h^{i-1}\|^2). \quad (5.3)$$

Here, the first term $\|\eta_h^i - \eta_h^{i-1}\|^2$ is fully computable, and by means of relation

$$\eta^i = \frac{1}{\gamma} (\alpha \text{div} \mathbf{u}^i - L p^i),$$

we obtain the estimate for the second and third terms:

$$\|\eta^i - \eta_h^i\|^2 \leq \frac{1}{2\gamma^2} (\alpha^2 \|\text{div}(e_{\mathbf{u}}^i)\|^2 + L^2 \|e_p^i\|^2) \stackrel{(4.12), (4.31)}{\leq} \frac{1}{2\gamma^2} \left(\alpha^2 \overline{M}_{u, \text{div}}^h(p_h^i) + L^2 \overline{M}_{p, L^2}^h(p_h^i) \right).$$

For simplicity, we exclude parameter γ by substituting $\gamma^2 = 2L$:

$$\|\eta^{i-1} - \eta_h^{i-1}\|^2 \leq \frac{1}{4L} (\alpha^2 \overline{M}_{u,\text{div}}^h(p_h^{i-1}) + L^2 \overline{M}_{p,L^2}^h(p_h^{i-1})). \quad (5.4)$$

Therefore, the estimate of $\|p - p^i\|_p^2$ can be represented as follows

$$\begin{aligned} \|p - p^i\|_p^2 \leq \overline{M}_P^i &:= \left(\frac{(C_F^F)^2 \beta}{\lambda_K \tau} + 1 \right) \frac{3q}{1-q^2} \left\{ \|\eta_h^i - \eta_h^{i-1}\|^2 \right. \\ &\left. + \frac{1}{4L} \left(\alpha^2 (\overline{M}_{u,\text{div}}^h(p_h^i) + \overline{M}_{u,\text{div}}^h(p_h^{i-1})) + L^2 (\overline{M}_{p,L^2}^h(p_h^i) + \overline{M}_{p,L^2}^h(p_h^{i-1})) \right) \right\}. \end{aligned} \quad (5.5)$$

Finally, by substituting $\lambda = \frac{\alpha^2}{2L}$ in (5.5), we arrive at (5.1). \square

Corollary 4. *Let conditions of Lemma 2 and Lemma 6 hold. Then, for $1 \leq m \leq i$, the estimate of the error incorporated in the pressure term on the i th iteration step has the alternative form*

$$\begin{aligned} \|p - p^i\|_p^2 \leq \overline{M}_p^{i,m}((\mathbf{u}, p)_h^{i-m}, (\boldsymbol{\tau}, \mathbf{z})_h^{i-m}, (\mathbf{u}, p)_h^i, (\boldsymbol{\tau}, \mathbf{z})_h^i) &:= \frac{3q^m}{1-q^{2m}} \left(\frac{(C_{\Sigma_D^F}^F)^2 \beta}{\lambda_K \tau} + 1 \right) \left(\|\eta_h^i - \eta_h^{i-m}\|^2 \right. \\ &+ \frac{\lambda}{2} (\overline{M}_{u,\text{div}}^h((\mathbf{u}, p)_h^i, (\boldsymbol{\tau}, \mathbf{z})_h^i) + \overline{M}_{u,\text{div}}^h((\mathbf{u}, p)_h^{i-m}, (\boldsymbol{\tau}, \mathbf{z})_h^{i-m})) \\ &\left. + \frac{L}{4} (\overline{M}_{p,L^2}^h(p_h^i, \mathbf{z}_h^i) + \overline{M}_{p,L^2}^h(p_h^{i-m}, \mathbf{z}_h^{i-m})) \right). \end{aligned} \quad (5.6)$$

The norm in the left-hand side of (5.3) can be alternatively estimated by the contractive estimate, which results into alternative error bound independent of the functional majorants. This result is presented below.

Lemma 7. *For any $p^i \in W_0$ approximating $p \in W_0$ in (2.8), the estimate of the error incorporated in the pressure term on the i th iteration step has the following form*

$$\begin{aligned} \|p - p^i\|_p^2 \leq \widehat{M}_p^i(\eta_h^1, \eta_h^0) &:= \left(\frac{(C_{\Sigma_D^F}^F)^2 \beta}{\lambda_K \tau} + 1 \right) \frac{3q^{2i-1}}{1-q^2} \\ &\left(\frac{\alpha^2}{\gamma^2} \overline{M}_{p,L^2}^h(p_h^1) + \frac{L^2}{\gamma^2} \overline{M}_{u,\text{div}}^h((\mathbf{u}, p)_h^1) + \|\eta^0 - \eta_h^0\|^2 + \|\eta_h^1 - \eta_h^0\|^2 \right), \end{aligned} \quad (5.7)$$

where

$$q = \frac{L}{\beta+L}, \quad \eta_h^i = \frac{\alpha}{\gamma} \text{div} \mathbf{u}_h^i - \frac{L}{\gamma} p_h^i, \quad L \geq \frac{\alpha^2}{2\lambda}, \quad \forall p_h^i \in W_{0h}, \quad \mathbf{u}_h^i \in \mathbf{V}_{0h},$$

and $\overline{M}_{u,\text{div}}^h$ and \overline{M}_{p,L^2}^h are defined in Corollaries 2 and 3. Parameters $\alpha, \beta, \lambda, \mu_f, C_{\Sigma_D^F}^F, \lambda_K$, and τ are characteristics of the semi-discrete Biot model (3.1) – (3.2).

Proof: We use inequality (5.2), to obtain

$$\|p - p^i\|_p^2 \leq \left(\frac{(C_{\Sigma_D^F}^F)^2 \beta}{\lambda_K \tau} + 1 \right) \frac{q}{1-q^2} \|\eta^i - \eta^{i-1}\|^2. \quad (5.8)$$

However, in this proof, we use contraction properties of sequence $\{\delta\eta^i\}$, to obtain

$$\|\eta^i - \eta^{i-1}\|^2 \leq q^{2(i-1)} \|\eta^1 - \eta^0\|^2 \leq q^{2(i-1)} (3\|\eta^1 - \eta_h^1\|^2 + 3\|\eta^0 - \eta_h^0\|^2 + 3\|\eta_h^1 - \eta_h^0\|^2) \quad (5.9)$$

where all terms on the right-hand side except $\|\eta^1 - \eta_h^1\|^2$ are computable. As in Lemma 3, $\|\eta^1 - \eta_h^1\|^2$ is controlled by combination of $\overline{M}_{p,L^2}^h(p_h^1, \mathbf{z}_h^1; \zeta)$ and $\overline{M}_{u,\text{div}}^h((\mathbf{u}, p)_h^1, \boldsymbol{\tau}_h^1, \mathbf{z}_h^1)$, i.e.,

$$\|\eta^1 - \eta_h^1\|^2 \leq \frac{\alpha^2}{\gamma^2} \|\text{div}(\mathbf{u}^1 - \mathbf{u}_h^1)\|^2 + \frac{L^2}{\gamma^2} \|p^1 - p_h^1\|^2 \leq \frac{\alpha^2}{\gamma^2} \overline{M}_{p,L^2}^h(p_h^1, \mathbf{z}_h^1; \zeta) + \frac{L^2}{\gamma^2} \overline{M}_{u,\text{div}}^h((\mathbf{u}, p)_h^1, \boldsymbol{\tau}_h^1, \mathbf{z}_h^1), \quad (5.10)$$

where right-hand side contains computable $\eta^0 := \frac{\alpha}{\gamma} \operatorname{div} \mathbf{u}^0 - \frac{L}{\gamma} p^0$. Combining (5.8), (5.9), and (5.10), we arrive at

$$\|p - p^i\|_p^2 \leq \left(\frac{(C_{\Sigma_D^F}^p)^2 \beta}{\lambda_{\text{K}} \tau} + 1 \right) \frac{3q^{2i-1}}{1-q^2} \left(\frac{\alpha^2}{\gamma^2} \overline{M}_{p,L^2}^h(p_h^1) + \frac{L^2}{\gamma^2} \overline{M}_{u,\operatorname{div}}^h((\mathbf{u}, p)_h^1) + \|\eta^0 - \eta_h^0\|^2 + \|\eta_h^1 - \eta_h^0\|^2 \right).$$

□

Error estimates for displacement term. To derive the upper bound for the error $\mathbf{u} - \mathbf{u}^i$ measured in terms of

$$\|\mathbf{u} - \mathbf{u}^i\|_{\mathbf{u}}^2 := \|\varepsilon(\mathbf{u} - \mathbf{u}^i)\|_{2\mu}^2 + \|\operatorname{div}(\mathbf{u} - \mathbf{u}^i)\|_{\lambda}^2, \quad (5.11)$$

we exploit the idea analogous to the one used to estimate the error in the pressure term.

Lemma 8. *For any $\mathbf{u}^i, \mathbf{u}^{i-1} \in \mathbf{V}_0$ approximating $\mathbf{u} \in \mathbf{V}_0$ in (2.7), the error in the displacement on the i th iteration step has the following form*

$$\begin{aligned} \|\mathbf{u} - \mathbf{u}^i\|_{\mathbf{u}}^2 &\leq \overline{M}_u^i((\mathbf{u}, p)_h^{i-1}, (\boldsymbol{\tau}, \mathbf{z})_h^{i-1}, (\mathbf{u}, p)_h^i, (\boldsymbol{\tau}, \mathbf{z})_h^i) := \left(1 + \frac{d\lambda}{2\mu}\right) \frac{3q^2}{1-q^2} \left(\|\eta_h^i - \eta_h^{i-1}\| \right. \\ &\quad \left. + \frac{\lambda}{2} (\overline{M}_{u,\operatorname{div}}^h((\mathbf{u}, p)_h^i, (\boldsymbol{\tau}, \mathbf{z})_h^i) + \overline{M}_{u,\operatorname{div}}^h((\mathbf{u}, p)_h^{i-1}, (\boldsymbol{\tau}, \mathbf{z})_h^{i-1})) \right) \\ &\quad \left. + \frac{L}{4} (\overline{M}_{p,L^2}^h(p_h^i, \mathbf{z}_h^i) + \overline{M}_{p,L^2}^h(p_h^{i-1}, \mathbf{z}_h^{i-1})) \right), \end{aligned} \quad (5.12)$$

where $\overline{M}_{u,\operatorname{div}}^h$ and \overline{M}_{p,L^2}^h are defined in Corollaries 2 and 3 for $\mathbf{z}_h^i, \mathbf{z}_h^{i-1} \in H_{\Sigma_N^p}(\Omega, \operatorname{div})$ and $\boldsymbol{\tau}_h^i, \boldsymbol{\tau}_h^{i-1} \in [\mathcal{T}_{\operatorname{Div}}(\Omega)]^{d \times d}$, respectively, $q = \frac{L}{\beta+L}$, and

$$\eta_h^i = \frac{\alpha}{\gamma} \operatorname{div} \mathbf{u}_h^i - \frac{L}{\gamma} p_h^i, \quad L = \frac{\alpha^2}{2\lambda}, \quad \forall p_h^i \in W_0, \mathbf{u}_h^i \in \mathbf{V}_0.$$

Parameters λ, μ, α are characteristics of the Biot model.

Proof: We consider

$$\|\mathbf{u} - \mathbf{u}^i\|_{\mathbf{u}}^2 \leq (2\mu + d\lambda) \|\varepsilon(e_{\mathbf{u}})\|^2, \quad (5.13)$$

where the right-hand side is controlled by the contractive term $\|\eta - \eta^i\|^2$, which follows from (3.9). Therefore, we obtain

$$\begin{aligned} \|\mathbf{u} - \mathbf{u}^i\|_{\mathbf{u}}^2 &\leq \frac{2\mu+d\lambda}{2\mu} \frac{q^2}{1-q^2} \|\eta^i - \eta^{i-1}\|^2 \\ &\leq \frac{2\mu+d\lambda}{2\mu} \frac{3q^2}{1-q^2} (\|\eta^i - \eta_h^i\|^2 + \|\eta^{i-1} - \eta_h^{i-1}\|^2 + \|\eta_h^i - \eta_h^{i-1}\|^2). \end{aligned} \quad (5.14)$$

Analogously to the proof of Lemma 6 (cf. (5.4)), the estimate for the second term in (5.14) results into

$$\begin{aligned} \|\mathbf{u} - \mathbf{u}^i\|_{\mathbf{u}}^2 &\leq \overline{M}_u^i := \left(1 + \frac{d\lambda}{2\mu}\right) \frac{3q^2}{1-q^2} \left(\|\eta_h^i - \eta_h^{i-1}\| \right. \\ &\quad \left. + \frac{1}{4L} \left(\alpha^2 (\overline{M}_{u,\operatorname{div}}^h(p_h^i, \mathbf{z}_h^i) + \overline{M}_{u,\operatorname{div}}^h(p_h^{i-1}, \mathbf{z}_h^{i-1})) + L^2 (\overline{M}_{p,L^2}^h(p_h^i, \mathbf{z}_h^i) + \overline{M}_{p,L^2}^h(p_h^{i-1}, \mathbf{z}_h^{i-1}))\right)\right). \end{aligned} \quad (5.15)$$

Again, by substituting $\lambda = \frac{\alpha^2}{2L}$ in (5.15), we arrive at (5.16). □

Corollary 5. *Let conditions of Lemma 2 and Lemma 8 hold. Then, for $1 \leq m \leq i$, the error in the displacement on the i th iteration step has the alternative form*

$$\begin{aligned} \|\mathbf{u} - \mathbf{u}^i\|_{\mathbf{u}}^2 &\leq \overline{M}_u^{i,m}((\mathbf{u}, p)_h^{i-m}, (\boldsymbol{\tau}, \mathbf{z})_h^{i-m}, (\mathbf{u}, p)_h^i, (\boldsymbol{\tau}, \mathbf{z})_h^i) := \left(1 + \frac{d\lambda}{2\mu}\right) \frac{3q^{2m}}{1-q^{2m}} \left(\|\eta_h^i - \eta_h^{i-m}\| \right. \\ &\quad \left. + \frac{\lambda}{2} (\overline{M}_{u,\operatorname{div}}^h((\mathbf{u}, p)_h^i, (\boldsymbol{\tau}, \mathbf{z})_h^i) + \overline{M}_{u,\operatorname{div}}^h((\mathbf{u}, p)_h^{i-m}, (\boldsymbol{\tau}, \mathbf{z})_h^{i-m})) \right) \\ &\quad \left. + \frac{L}{4} (\overline{M}_{p,L^2}^h(p_h^i, \mathbf{z}_h^i) + \overline{M}_{p,L^2}^h(p_h^{i-m}, \mathbf{z}_h^{i-m})) \right). \end{aligned} \quad (5.16)$$

Analogously, contraction properties can be exploited to derive an alternative bound of the error $\mathbf{u} - \mathbf{u}^i$.

Lemma 9. *For any $\mathbf{u}^i \in \mathbf{V}_0$ approximating $\mathbf{u} \in \mathbf{V}_0$ in (2.7), the error in the displacement on the i th iteration step has the following form*

$$\|\mathbf{u} - \mathbf{u}^i\|_{\mathbf{u}}^2 \leq \widetilde{M}_u^i(\eta_h^1, \eta_h^0) := \frac{2\mu+d\lambda}{2\mu} \frac{3q^{2i}}{1-q^2} \left(\frac{\alpha^2}{\gamma^2} \overline{M}_{p,L^2}^h(p_h^1) + \frac{L^2}{\gamma^2} \overline{M}_{u,\text{div}}^h((\mathbf{u}, p)_h^1) + \|\eta^0 - \eta_h^0\|^2 + \|\eta_h^1 - \eta_h^0\|^2 \right), \quad (5.17)$$

where

$$q = \frac{L}{\beta+L}, \quad \eta_h^i = \frac{\alpha}{\gamma} \text{div} \mathbf{u}_h^i - \frac{L}{\gamma} p_h^i, \quad L = \frac{\alpha^2}{2\lambda}, \quad \forall p_h^i \in W_0, \mathbf{u}_h^i \in \mathbf{V}_0,$$

and $\overline{M}_{u,\text{div}}^h$ and \overline{M}_{p,L^2}^h are defined in Corollaries 2 and 3. Parameters λ, μ, α are characteristics of the Biot model.

Proof: The derivation comprises of combining

$$\|\mathbf{u} - \mathbf{u}^i\|_{\mathbf{u}}^2 \leq \frac{2\mu+d\lambda}{2\mu} \frac{q^2}{1-q^2} \|\eta^i - \eta^{i-1}\|^2, \quad (5.18)$$

(5.9), and (5.10). □

General estimate for the error in the iterative coupling scheme. Derivation of the reliable estimate for the error in the pressure approximation reconstructed on the i th iteration is based on the combination of two different approaches, i.e., estimates for contractive mapping used for iterative methods and functional error estimates. Theorem 2 presents an upper bound of the error in the pressure term, which combines the above-mentioned techniques.

Theorem 2. *For any $p_h^i \in W_0$ and $\mathbf{u}_h^i \in \mathbf{V}_0$ that form a contraction relative to $p_h^{i-1} \in W_0$ and $\mathbf{u}_h^{i-1} \in \mathbf{V}_0$, we have the estimates*

$$\begin{aligned} \|e_p\|_p^2 &\leq \overline{M}_p := 2 \left(\overline{M}_p^h(p_h^i, \mathbf{z}_h^i) + \min \left\{ \overline{M}_p^i, \overline{M}_p^{i,m}, \widetilde{M}_p^i \right\} \right), \\ \|e_u\|_{\mathbf{u}}^2 &\leq \overline{M}_u := 2 \left(\overline{M}_u^h((\mathbf{u}, p)_h^i, (\boldsymbol{\tau}, \mathbf{z})_h^i) + \min \left\{ \overline{M}_u^i, \overline{M}_u^{i,m}, \widetilde{M}_u^i \right\} \right). \end{aligned}$$

Here, $\overline{M}_p^h, \overline{M}_p^i, \overline{M}_p^{i,m}$, and \widetilde{M}_p^i are defined in Lemmas 3, 6, Corollary 4, and Lemma 7, whereas $\overline{M}_u^h, \overline{M}_u^i$, and \widetilde{M}_u^i are presented by Lemmas 5, 8, Corollary 5, and Lemma 9, respectively, where $p_h^{i-1} \in W_0, \mathbf{u}_h^{i-1} \in \mathbf{V}_0, \mathbf{z}_h^i, \mathbf{z}_h^{i-1} \in H_{\Sigma_N^p}(\Omega, \text{div}), \boldsymbol{\tau}_h^i, \boldsymbol{\tau}_h^{i-1} \in [\mathcal{T}_{\text{Div}}(\Omega)]^{d \times d}$, and parameter $\zeta \geq 0$.

Proof: To decompose the error $\|e_p\|_p^2$ in two parts, we apply the triangle inequality

$$\|e_p\|_p^2 = \|p - p_h^i\|_p^2 \leq 2 \left(\|p - p^i\|_p^2 + \|p^i - p_h^i\|_p^2 \right). \quad (5.19)$$

The first term in the right-hand side of (5.19) is bounded by (5.1) from Lemma 6, whereas the second term is controlled by (4.2) from Lemma 3. Analogously, by using the triangle rule, we obtain

$$\|e_u\|_{\mathbf{u}}^2 = \|\mathbf{u} - \mathbf{u}_h^i\|_{\mathbf{u}}^2 \leq 2 \left(\|\mathbf{u} - \mathbf{u}^i\|_{\mathbf{u}}^2 + \|\mathbf{u}^i - \mathbf{u}_h^i\|_{\mathbf{u}}^2 \right). \quad (5.20)$$

The first term in the right-hand side of (5.20) is controlled by (5.16), whereas the estimate of the second term follows from (4.16). □

Theorem 3. *For any $p_h^i \in W_0$ and $\mathbf{u}_h^i \in \mathbf{V}_0$, we have the estimates*

$$[e_p, e_u] \leq \overline{M} := \overline{M}_p + \overline{M}_u,$$

where \overline{M}_p and \overline{M}_u are defined in Theorem 2.

6. Numerical example

The numerical properties of above estimates are explained in the series of the following numerical examples. We take two tests where we begin with a manufactured solution for the pressure and displacement. These tests pertain to different values of the contraction coefficient q in the fixed stress scheme and study the efficiency of the error estimators. For each of the two tests, we consider both parameters that are academic as well as repeat them for more realistic parameters of the material properties (permeability, Lamé coefficients etc). We solve the Biot model at each time step using the fixed stress scheme by choosing different mesh sizes and time steps. Moreover, we also vary the finite element pairs used for solving the problem. All these variations, including material properties, discretization parameters, and the finite element pairs allow us to study the performance of the estimators and show their robustness.

Our approach is to compute the approximations of the pressure and displacement for the test cases and study the convergence of this to the exact solution. The errors are computed by employing different norms including the combination of pressure and displacement as well the individual ones in both L^2 and the energy norms. We choose a time and a spatial mesh size and at this discrete time, we fix the number of fixed stress iterations and study the convergence. The majorants \overline{M}_p^h and \overline{M}_u^h are obtained via minimisations w.r.t. to the auxiliary functions. To characterise the efficiency of all the above mentioned error estimators, we use the efficiency index defined as $I_{\text{eff}} := \overline{M}/\|e\|^2$, where \overline{M} is a chosen majorant and $\|e\|^2$ is error measured in the corresponding error norm. We study the individual contributions of the different terms in the majorants, namely the dual term and reliability/equilibration term. The first one allows us to study the efficiency as the error indicators and the small contribution of the second one ensures the reliability of the total error bounds. This is studied for the different majorants, the one for the discretization error and for the iterative ones and for the different choices of error norms.

Example 1. Simplified parameters. Let $\Omega := (0, 1)^2 \in \mathbb{R}^2$, $T = 10$. The exact solution of (1.1) is defined as

$$\mathbf{u}(x, y, t) := tx(1-x)y(1-y)[1, 1]^T \quad \text{and} \quad p(x, y, t) := tx(1-x)y(1-y).$$

The Lamé parameters are $\mu = \lambda_{\text{vol}} = 1$, which leads to $\lambda_{\text{plane}} = \frac{2\lambda_{\text{vol}}\mu}{\lambda_{\text{vol}}+2\mu} = \frac{2}{3}$. We set $\alpha = \beta = 1$, $C_F = \frac{1}{\sqrt{2}\pi}$, and \mathbb{K} [mD/cP] is a unit tensor. From the parameters above, it follows that $L = \frac{\alpha^2}{2(\lambda+2\mu/d)} = 0.3$ and $q = \frac{L}{\beta+L} = \frac{3}{13} \approx 0.23077$. Taking into account that the error estimates depend on the term $\frac{q^2}{(1-q^2)}$, which goes to infinity as q goes to 1, the efficiency of the resulting \overline{M}_u and \overline{M}_p drastically depends on the value of q . In this particular example, the ratio $\frac{q^2}{(1-q^2)} = 0.05625$ is relatively small, which prevents \overline{M}_u^i and \overline{M}_p^i overestimating the errors.

$i = 1, \dots, I$	$\ e_p\ ^2$	\overline{M}_p^h	$\ e_p\ _\beta^2$	\overline{M}_{p,L^2}^h	$\ e_u\ ^2$	\overline{M}_u^h	$\ \text{div}e_u\ _\lambda^2$	$\overline{M}_{u,\text{div}}^h$
(a) $N = 10$, $[t_9, t_{10}]$, $\tau = 1.0$								
1	1.2868e-02	—	2.4070e-04	—	2.0722e-04	—	5.1044e-05	—
2	1.8733e-04	1.8732e-04	4.7759e-09	8.9032e-06	1.8687e-04	4.9549e-04	4.4544e-05	1.0618e-04
3	1.8731e-04	—	2.0666e-09	—	1.8687e-04	—	4.4544e-05	—
4	1.8731e-04	1.8738e-04	2.0481e-09	8.9060e-06	1.8687e-04	4.9549e-04	4.4544e-05	1.0618e-04
5	1.8731e-04	1.8738e-04	2.0479e-09	8.9060e-06	1.8687e-04	4.9549e-04	4.4544e-05	1.0618e-04
(b) $N = 10^2$, $[t_{99}, t_{100}]$, $\tau = 0.1$								
1	7.0040e-01	—	1.1032e-01	—	1.5274e-03	—	4.6795e-04	—
2	1.7443e-04	1.2920e-04	1.0388e-05	3.9462e-05	1.8690e-04	5.0505e-04	4.4558e-05	1.0823e-04
3	1.3128e-04	—	8.8865e-08	—	1.8687e-04	—	4.4544e-05	—
4	1.3113e-04	1.3111e-04	1.7743e-08	4.0047e-05	1.8687e-04	4.9275e-04	4.4544e-05	1.0559e-04
5	1.3113e-04	1.3112e-04	1.5374e-08	4.0049e-05	1.8687e-04	4.9276e-04	4.4544e-05	1.0559e-04

Table 1: *Example 1.* Errors and majorants w.r.t. the iteration steps for $h = \frac{1}{64}$ and $I = 5$ (both values are measured relative to the increment in $\|p\|_p^2$ and $\|\mathbf{u}\|_u^2$ on the N th time step).

First, we generate approximations employing 10 time steps (where the total number of steps in time is denoted by N) with corresponding size of the step $\tau = 1.0$ and spatial mesh-size $h = \frac{1}{64}$ using standard \mathbb{P}_1 (polynomial/lagrangian first-order) finite elements (see (6.7)). Let I denote the number of iterations to solve (3.4)–(3.5) on each time-step; we consider $I = 5$ for this discretization. Table 1 illustrates the convergence of the errors in \mathbf{u} and p w.r.t. the iteration steps $i = 1, \dots, I$ for the time-interval $[t_9, t_{10}] = [9.0, 10.0]$.

optimization step	ζ	$\ e_p\ ^2$	\overline{M}_p^h	\overline{m}_d^2	\overline{m}_{eq}^2	$I_{\text{eff}} := \overline{M}_p^h / \ e_p\ ^2$
0	0.4359	1.87e-04	4.55e-04	1.87e-04	8.06e-05	1.5589
1	0.0045	1.87e-04	2.69e-04	1.87e-04	1.53e-08	1.1983
2	0.0002	1.87e-04	1.88e-04	1.87e-04	1.67e-08	1.0023

Table 2: *Example 1.* Decrease of the values of the parameter ζ and the majorant \overline{M}_p^h , as well as the terms \overline{m}_d^2 and \overline{m}_{eq}^2 it contains, w.r.t. the number of optimization cycles.

The values of \overline{M}_p^h and \overline{M}_u^h are obtained by minimization of each functional w.r.t. to auxiliary functions. For instance, the functional estimate to control the error in variable p

$$\overline{M}_p^h(p_h^i, \mathbf{z}_h^i; \zeta) := (1 + \zeta) \|\mathbf{r}_d(p_h^i, \mathbf{z}_h^i)\|_{\mathbb{K}_\tau^{-1}}^2 + (1 + \frac{1}{\zeta}) C_\Omega^p \left(2 \|\mathbf{r}_{eq}(p_h^i, \mathbf{z}_h^i)\|_\Omega^2 + 2\gamma^2 q^{2(i-1)} \|\eta^0 - \eta_h^0\|^2 + \|\mathbf{z}_h^i \cdot \mathbf{n}\|_{\Sigma_N^p}^2 \right) \quad (6.1)$$

is minimized w.r.t. the function \mathbf{z}_h^i and parameter ζ . The results of this optimization procedure are listed in Table 2. We see that only two iterations are enough to achieve good efficiency $I_{\text{eff}} := \overline{M}_p^h / \|e_p\|^2 = 1.0023$. In Table 2, we see the decrease of the dual term $\overline{m}_d^2 := \|\mathbf{r}_d(p_h^i, \mathbf{z}_h^i)\|_{\mathbb{K}_\tau^{-1}}^2 = \|\mathbf{z}_h^i - \mathbb{K}_\tau \nabla p_h^i\|_{\mathbb{K}_\tau^{-1}}^2$ as well as the reliability/equilibration term of the majorant $\overline{m}_{eq}^2 := \|\mathbf{r}_{eq}(p_h^i, \mathbf{z}_h^i)\|_\Omega^2 = \|\tilde{g} - \gamma \eta_h^{i-1} - (\beta + L)p_h^i + \text{div} \mathbf{z}_h^i\|_\Omega^2$. In order to achieve the desired efficiency in the error estimate, the reliability term must be several orders of magnitude less than the dual one, which is satisfied in this case.

Analogous minimization is performed for the majorant \overline{M}_u^h . After minimization, the terms $\overline{m}_{d,K}^2$ and $\overline{m}_{d,\lambda,\mu}^2$ become very close to the true errors $\|e_p\|^2$ and $\|e_u\|^2$, respectively, and can be used as error indicators for the local error distribution over the computational domain. To confirm that, Figure 1 presents the distribution of the errors and indicators (generated by majorants) w.r.t. to the numbered finite element cells. On the right side of Figure 1, we depict $\|e_p\|^2$ and $\overline{m}_{d,K}^2 := \|\mathbf{r}_{d,K}(p_h^i, \mathbf{z}_h^i)\|^2$ and on the left side the error in \mathbf{u} measured in terms of $\|e_u\|^2$ as well as the indicator $\overline{m}_{d,\mu,\lambda}^2 := \|\mathbf{r}_{d,\mu,\lambda}(\mathbf{u}_h^i, \boldsymbol{\tau}_h^i)\|^2$ w.r.t. to the numbered finite element cells. To depict the error green marker is used, whereas for the majorant the red color is chosen. We see that the indicator produces quantitatively efficient error indicator. First, let us assume that the error bounds \overline{M}_p^h and \overline{M}_{p,L^2}^h , as well as \overline{M}_u^h and $\overline{M}_{u,\text{div}}^h$ are reconstructed only on the 4th and 5th steps to calculate \overline{M}_u^i and \overline{M}_p^i for $i = 5$ (using (5.1) and (5.16)). Let $\|e_p^{(n)}\|^2$ and $\|e_u^{(n)}\|^2$, $n = 1, \dots, N$ correspond to the error increments corresponding to the n th time-step. The contribution of the majorants of discretization errors and the iterative majorant on the N th time step are of the same magnitude, i.e.,

$$\overline{M}_p^{h,(N)} = 1.8736\text{e-}04, \quad \overline{M}_p^{i,(N)} = 3.0550\text{e-}04, \quad \overline{M}_u^{h,(N)} = 4.9549\text{e-}04, \quad \overline{M}_u^{i,(N)} = 3.2025\text{e-}05.$$

Then, N th increment of both total errors and corresponding majorants for the pressure as well as the displacement respectively are as follows:

$$\begin{aligned} \|e_p^{(N)}\|^2 &= 4.8652\text{e-}05, & \overline{M}_p^{(N)} &= 2.5603\text{e-}04, & I_{\text{eff}}(\overline{M}_p^{(N)}) &= 2.29 \quad \text{and} \\ \|e_u^{(N)}\|^2 &= 4.8536\text{e-}05, & \overline{M}_u^{(N)} &= 2.7403\text{e-}04, & I_{\text{eff}}(\overline{M}_u^{(N)}) &= 2.38, \end{aligned}$$

making the general error, majorant, and corresponding efficiency index contributions the following

$$[(e_u^{(N)}, e_p^{(N)})]^2 = 4.8559\text{e-}04, \quad \overline{M}^{(N)} = 9.9944\text{e-}05, \quad I_{\text{eff}}(\overline{M}^{(N)}) = 2.36.$$

If instead of 4th and 5th iterations we use 2nd and 5th to compute $\overline{M}_u^{i,m,(N)}$ and $\overline{M}_p^{i,m,(N)}$ (using $m = 3$ in (3.10) and (3.11)). Then contribution of iterative majorants is

$$\overline{M}_p^{i,m,(N)} = 5.0348\text{e-}06 \quad \text{and} \quad \overline{M}_u^{i,m,(N)} = 2.8107\text{e-}08.$$

Then, the accumulated overall time steps values of the relative errors and majorants are

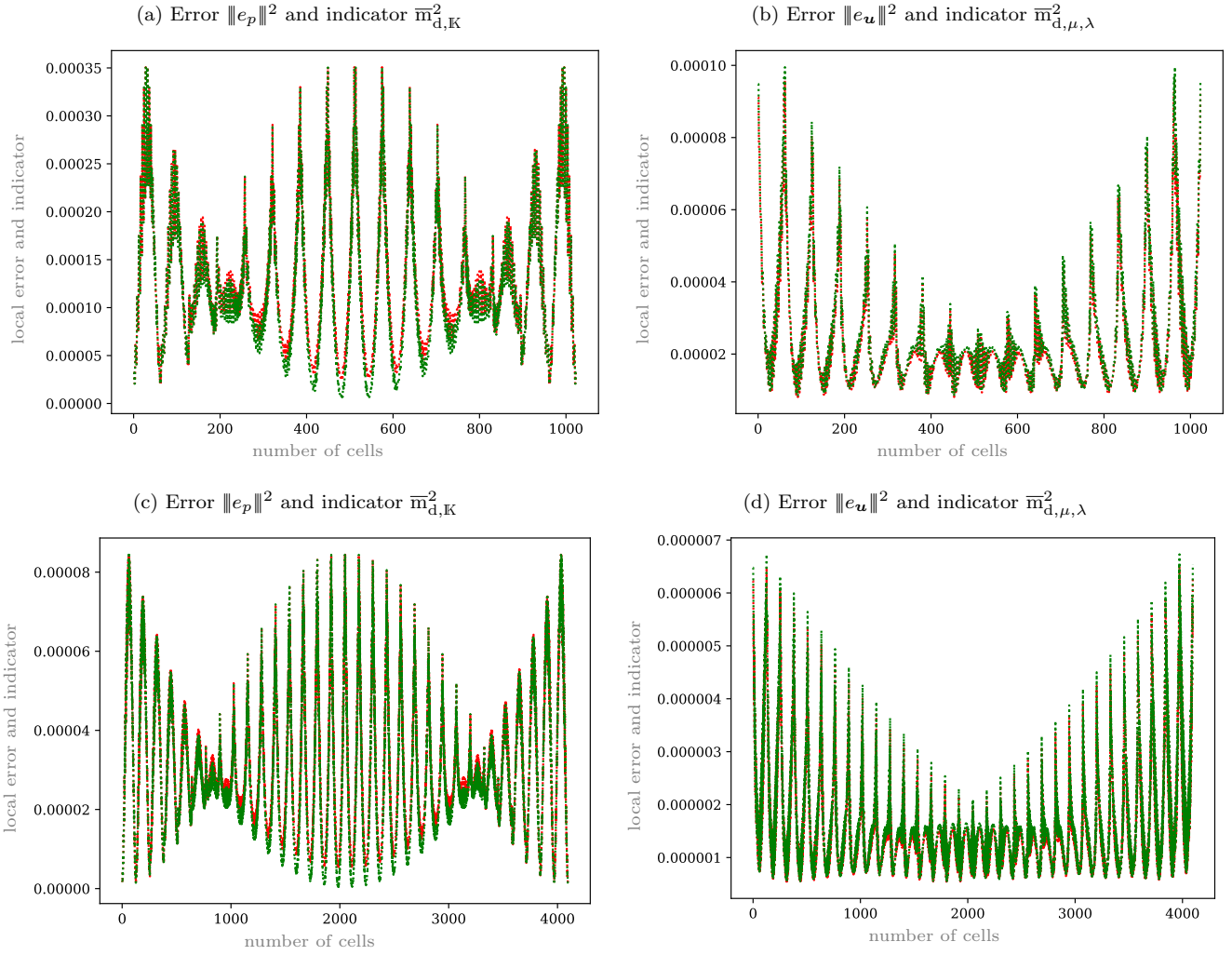


Figure 1: *Example 1.* (a),(c) Local distribution of error $\|e_p\|^2$ in red and error indicator $\overline{m}_{d,K}^2$ generated by the majorant \overline{M}_p^h in green and (b),(d) local distribution of error $\|e_u\|^2$ in red and error indicator $\overline{m}_{d,\mu,\lambda}^2$ generated by the majorant \overline{M}_u^h in green. The distributions are depicted w.r.t. the numbered finite element cells of the uniform meshes with (a)–(b) $h = 1/32$ and (c)–(d) $h = 1/64$.

$$\|e_p\|^2 = \sum_{n=1}^N \|e_p^{(n)}\|^2 = 1.8731\text{e-}04, \quad \|e_u\|^2 = \sum_{n=1}^N \|e_u^{(n)}\|^2 = 1.8687\text{e-}04, \quad \text{and}$$

$$\overline{M}_p = \sum_{n=1}^N \overline{M}_p^{(n)} = 3.8479\text{e-}04, \quad \overline{M}_u = \sum_{n=1}^N \overline{M}_u^{(n)} = 9.9104\text{e-}04,$$

respectively, with corresponding efficiency indices over the whole time interval are summarised in Table 3(a). The results are presented corresponding to meshes with two different mesh-sizes h and τ . As the caption highlights, all these values are obtained for the auxiliary functions are reconstructed by the following finite elements $\mathbf{z}_h^i \in \text{RT}_1$ and $\boldsymbol{\tau}_h^i \in [\text{P}_2]^{2 \times 2}$, which is an order higher than usual choice of the finite element approximation spaces for the fluxes and stresses in mixed formulations. However, it is important to obtain better accuracy of the error bounds. To emphasize this importance, Table 4 lists the results obtained for cases, when different finite elements pairs for auxiliary functions are used, i.e., (a) $\mathbf{z}_h^i \in \text{RT}_0$ and $\boldsymbol{\tau}_h^i \in [\text{P}_2]^{2 \times 2}$ or (b) $\mathbf{z}_h^i \in \text{RT}_1$ and $\boldsymbol{\tau}_h^i \in [\text{P}_1]^{2 \times 2}$.

Assume now that $N = 10^3$. Analogously, we consider the last time-step $[t_{999}, t_{1000}]$ with mesh-size $h = \frac{1}{64}$. Table

h	$\ e_p\ ^2$	\overline{M}_p	$\ e_u\ ^2$	\overline{M}_u	$[(e_u, e_p)]^2$	\overline{M}	$I_{\text{eff}}(\overline{M})$
(a) $N = 10, \quad \tau = 1.0$							
$1/4$	4.8163e-02	1.0299e-01	4.8035e-02	2.6402e-01	6.1827e-02	2.9352e-01	2.18
$1/8$	1.2006e-02	2.4971e-02	1.1977e-02	6.4119e-02	1.5415e-02	7.1270e-02	2.15
$1/16$	2.9981e-03	6.1776e-03	2.9909e-03	1.5899e-02	3.8495e-03	1.7668e-02	2.14
$1/32$	7.4930e-04	1.5398e-03	7.4752e-04	3.9663e-03	9.6209e-04	4.4072e-03	2.14
$1/64$	1.8731e-04	3.8479e-04	1.8687e-04	9.9104e-04	2.4050e-04	1.1012e-03	2.14
(b) $N = 10^2, \quad \tau = 0.1$							
$1/4$	3.4606e-02	6.9224e-02	4.8035e-03	2.6245e-02	6.2192e-03	2.9077e-02	2.16
$1/8$	8.4602e-03	1.7171e-02	1.1977e-03	6.3753e-03	1.5438e-03	7.0778e-03	2.14
$1/16$	2.1022e-03	4.2867e-03	2.9909e-04	1.5809e-03	3.8509e-04	1.7563e-03	2.14
$1/32$	5.2472e-04	1.0754e-03	7.4752e-05	3.9441e-04	9.6218e-05	4.3841e-04	2.13
$1/64$	1.3113e-04	2.7329e-04	1.8687e-05	9.8551e-05	2.4051e-05	1.0973e-04	2.14
(c) $N = 10^3, \quad \tau = 0.01$							
$1/4$	1.0880e-02	3.5205e-02	4.8035e-04	2.6104e-03	6.5839e-04	3.1865e-03	2.20
$1/8$	2.2543e-03	8.7416e-03	1.1977e-04	6.3403e-04	1.5666e-04	7.7708e-04	2.23
$1/16$	5.3424e-04	2.1800e-03	2.9909e-05	1.5722e-04	3.8652e-05	1.9289e-04	2.23
$1/32$	1.3172e-04	5.4464e-04	7.4752e-06	3.9223e-05	9.6307e-06	4.8135e-05	2.24
$1/64$	3.2816e-05	1.3621e-04	1.8687e-06	9.8005e-06	2.4056e-06	1.2029e-05	2.24

Table 3: *Example 1.* Convergence of errors and majorants w.r.t. the different choice of spatial mesh sizes h and time steps τ (measured relatively w.r.t. $\|p\|_p^2$ and $\|u\|_u^2$). For all the cases, the auxiliary functions are reconstructed by the following finite elements $\mathbf{z}_h^i \in \text{RT}_1$ and $\tau_h^i \in [\text{P}_2]^{2 \times 2}$.

h	$\ e_p\ ^2$	\overline{M}_p	$\ e_u\ ^2$	\overline{M}_u	$[(e_u, e_p)]^2$	\overline{M}	$I_{\text{eff}}(\overline{M})$
(a) $\mathbf{z}_h^i \in \text{RT}_0, \quad \tau_h^i \in [\text{P}_2]^{2 \times 2}$							
$1/4$	1.5184e-02	9.9777e-02	1.2934e-02	7.3430e-02	2.8119e-02	1.7321e-01	2.48
$1/8$	3.7854e-03	2.5695e-02	3.2249e-03	1.7884e-02	7.0102e-03	4.3579e-02	2.49
$1/16$	9.4525e-04	6.4694e-03	8.0535e-04	4.4381e-03	1.7506e-03	1.0907e-02	2.50
$1/32$	2.3624e-04	1.6202e-03	2.0128e-04	1.1074e-03	4.3752e-04	2.7276e-03	2.50
$1/64$	5.9055e-05	4.0529e-04	5.0316e-05	2.7672e-04	1.0937e-04	6.8201e-04	2.50
(b) $\mathbf{z}_h^i \in \text{RT}_1, \quad \tau_h^i \in [\text{P}_1]^{2 \times 2}$							
$1/4$	1.5184e-02	2.3151e-01	1.2934e-02	2.9586e-01	2.8119e-02	5.2737e-01	4.33
$1/8$	3.7854e-03	5.9349e-02	3.2249e-03	7.6502e-02	7.0102e-03	1.3585e-01	4.40
$1/16$	9.4525e-04	1.4935e-02	8.0535e-04	1.9301e-02	1.7506e-03	3.4236e-02	4.42
$1/32$	2.3624e-04	3.7402e-03	2.0128e-04	4.8369e-03	4.3752e-04	8.5771e-03	4.43
$1/64$	5.9055e-05	9.3545e-04	5.0316e-05	1.2100e-03	1.0937e-04	2.1454e-03	4.43

Table 4: *Example 1.* Convergence of errors and majorants w.r.t. the different choice of approximation spaces for \mathbf{z}_h^i and τ_h^i (measured relatively w.r.t. $\|p\|_p^2$ and $\|u\|_u^2$). For all the cases, simulation is performed for the discretization with $\tau = 1.0$.

5 illustrates the convergence of the errors in \mathbf{u} and p w.r.t. iteration steps (in this case, we consider $I = 10$). For considered $\tau = 0.01$, the contribution of the majorants of the discretization errors and the iterative majorant on the pressure variable differ in magnitude, i.e.,

$$\overline{M}_p^{h,(N)} = 6.6685e-05, \quad \overline{M}_p^{i,(N)} = 3.0410e-02, \quad \overline{M}_u^{h,(N)} = 4.9003e-04, \quad \overline{M}_u^{i,(N)} = 3.1551e-05.$$

These are the results obtained considering two last subsequent iteration steps with $q = 0.2307$ that correspond to $\frac{3q}{1-q^2} \left(\frac{(C_{\Sigma D}^F)^2 \beta}{\lambda_K \tau} + 1 \right) = 7.0973$. Such a difference in $\overline{M}_p^{h,(N)}$ and $\overline{M}_p^{i,(N)}$ results in the error majorant with the efficiency index $I_{\text{eff}}(\overline{M}_p^{(N)}) = 43.10$. However, if we assume, say, the third and tenth steps to be subsequent ones, it provides a better contractive parameter $\tilde{q} := q^7 = 3.4853e-05$ and improves the efficiency index of error estimates corresponding to pressure and displacement by approximately 21.12 and 1.03 times, respectively, i.e.,

$$\overline{M}_p^{i,m,(N)} = 1.4154e-06 \quad \text{and} \quad \overline{M}_u^{i,m,(N)} = 2.2179e-13$$

$i = 1, \dots, I$	$\ e_p\ ^2$	\overline{M}_p^h	$\ e_p\ _\beta^2$	\overline{M}_{p,L^2}^h	$\ e_u\ ^2$	\overline{M}_u^h	$\ \text{div}e_u\ _\lambda^2$	$\overline{M}_{u,\text{div}}^h$
1	5.8753e+00	—	3.5255e+00	—	1.7140e-02	—	5.2771e-03	—
2	3.0103e-03	—	1.3101e-03	—	1.9054e-04	—	4.5713e-05	—
3	5.5125e-05	8.6791e-05	1.6877e-05	5.7961e-05	1.8688e-04	4.9901e-04	4.4550e-05	1.0693e-04
4	3.3497e-05	—	5.9589e-07	—	1.8687e-04	—	4.4544e-05	—
...
8	3.2817e-05	—	3.8002e-08	—	1.8687e-04	—	4.4544e-05	—
9	3.2817e-05	6.6685e-05	3.7904e-08	4.4534e-05	1.8687e-04	4.9003e-04	4.4544e-05	1.0501e-04
10	3.2817e-05	6.6685e-05	3.7889e-08	4.4534e-05	1.8687e-04	4.9003e-04	4.4544e-05	1.0501e-04

Table 5: *Example 1.* Errors errors and majorants w.r.t. the iteration steps for $I = 7$, $h = \frac{1}{64}$, $N = 10^3$, $[t_{999}, t_{1000}]$, $\tau = 0.01$ (both values are measured relative to the increment in $\|p\|_p^2$ and $\|u\|_u^2$ on the N th time step).

This yields

$$\begin{aligned} \|e_p^{(N)}\|^2 &= 9.8302e-08, & \overline{M}_p^{(N)} &= 4.0799e-07, & I_{\text{eff}}(\overline{M}_p^{(N)}) &= 2.04 & \text{ and} \\ \|e_u^{(N)}\|^2 &= 5.5976e-09, & \overline{M}_u^{(N)} &= 2.9358e-08, & I_{\text{eff}}(\overline{M}_u^{(N)}) &= 2.29. \end{aligned}$$

The accumulated values of the pressure error, majorant, and corresponding efficiency index over the whole time interval are as follows:

$$\|e_p\|^2 = 3.2816e-05, \quad \overline{M}_p = 1.3621e-04, \quad \text{and} \quad I_{\text{eff}}(\overline{M}_p) = 2.04.$$

For the displacement, we observe

$$\|e_u\|^2 = 1.8687e-06, \quad \overline{M}_u = 9.8005e-06, \quad \text{and} \quad I_{\text{eff}}(\overline{M}_u) = 2.29.$$

This yields the total values $[(e_u, e_p)] = 2.4056e-06$ and $\overline{M} = 1.2029e-05$ with efficiency index $I_{\text{eff}} := \frac{\overline{M}}{[(e_u, e_p)]} = 2.24$. The latter values are included in Table 3(c). They illustrate the accumulated values of the errors and majorant over the whole time interval. We see that even with the decreasing τ , which scales the permeability tensor \mathbb{K} , the efficiency of total error estimates stays rather robust.

We note here, that each increment of $\overline{M}_p^{(N)}$ and $\overline{M}_u^{(N)}$ can be computed using \widetilde{M}_p^i and \widetilde{M}_u^i , which does not require computation of the majorant of discretization errors $\overline{M}_p^{h,(N)}$ and $\overline{M}_u^{h,(N)}$ on iteration steps $i-1$ or $i-m$ and, as consequence, their minimization w.r.t. the auxiliary functions \mathbf{z}_h^i and $\boldsymbol{\tau}_h^i$, respectively. Moreover, the values \widetilde{M}_p^i and \widetilde{M}_u^i are orders of magnitude smaller than $\overline{M}_p^{i,m,(N)}$ and $\overline{M}_u^{i,m,(N)}$, i.e., $\widetilde{M}_p^i = 7.0735e-10$ and $\widetilde{M}_u^i = 7.3390e-13$. Such values automatically minimize the contribution of iterative estimates into $\overline{M}_p^{h,(N)}$ and $\overline{M}_u^{h,(N)}$ and even further improves their efficiency.

Realistic parameters. Let us assume now more realistic parameters in the above example (similar to those taken from [66] and [59]). Let exact pressure be scaled as follows: $p(x, y, t) = 10^8 x(1-x)y(1-y)t$. The permeability tensor divided by fluid viscosity is taken as $\mathbb{K} = 100\mathbb{I}$ [mD/cP], fluid compressibility fixed to $4.7 \cdot 10^{-7}$ [psi $^{-1}$], and initial porosity ϕ_0 is assumed to be 0.2. The Biot and bulk modulus are $M = 1.65 \cdot 10^{10}$ [Pa] and $E = 0.594 \cdot 10^9$ [Pa], respectively. That results into $\beta = \frac{1}{M} + c_f \phi_0 = 9.406 \cdot 10^{-8}$, which, in turn, yields considerable small $L = \frac{\alpha^2}{2(\lambda+2\mu/d)} = 1.35 \cdot 10^{-9}$. Such a tuning parameter generates instantaneous convergence of iterative scheme with contractive parameter $q = \frac{L}{\beta+L} = 6.73 \cdot 10^{-12}$. The resulting errors and corresponding estimates are summarised in Table 6 (for $\tau = 0.1$ and difference spacial mesh-sizes h). For such q , even one iteration is enough for convergence. However, one can consider two to five iterations to improve the efficiency of the majorant. The efficiency indices obtained here confirm the efficiency of obtained majorants also for parameters closed to those used in engineering applications.

Example 2. Simplified parameters. Let $\Omega := (0, 1)^2 \in \mathbb{R}^2$, $T = 10$. The exact solution of (1.1) is defined as

$$\mathbf{u}(x, y, t) := \begin{bmatrix} t(x^2 + y^2) \\ t(x + y) \end{bmatrix} \quad \text{and} \quad p(x, y, t) := tx(1-x)y(1-y).$$

h	$\ e_p\ ^2$	\overline{M}_p	$\ e_u\ ^2$	\overline{M}_u	$[(e_u, e_p)]^2$	\overline{M}	$I_{\text{eff}}(\overline{M})$
$1/4$	5.0067e-02	3.9082e-01	4.7948e-03	8.3004e-02	5.0067e-02	3.9082e-01	2.79
$1/8$	1.2576e-02	9.6727e-02	1.2024e-03	2.0992e-02	1.2576e-02	9.6727e-02	2.77
$1/16$	3.1461e-03	2.3977e-02	3.0070e-04	5.2587e-03	3.1461e-03	2.3977e-02	2.76
$1/32$	7.8664e-04	5.9649e-03	7.5179e-05	1.3152e-03	7.8664e-04	5.9649e-03	2.75
$1/64$	1.9667e-04	1.4874e-03	1.8795e-04	3.2882e-03	1.9667e-04	1.4874e-03	2.75

Table 6: *Example 1.* Convergence of errors and majorants w.r.t. the different choice of spatial mesh sizes (measured relatively w.r.t. $\|p_h^i\|_p^2$ and $\|\mathbf{u}_h^i\|_u^2$) for $N = 100$ and $\tau = 0.1$.

# it.	$\ e_p\ ^2$	\overline{M}_p^h	$\ e_p\ _\beta^2$	\overline{M}_{p,L^2}^h	$\ e_u\ ^2$	\overline{M}_u^h	$\ \text{div}e_u\ _\lambda^2$	$\overline{M}_{u,\text{div}}^h$
(a) $N = 10, \quad \tau = 1.0$								
1	5.3962e+00	—	2.9479e-02	—	8.4773e-04	—	1.2996e-03	—
...
5	1.9553e-04	—	2.4696e-10	—	8.5024e-06	—	9.8152e-06	—
6	1.9553e-04	1.9559e-04	2.6065e-10	9.2250e-06	8.5024e-06	2.6115e-05	9.8152e-06	2.3448e-05
...
10	1.9553e-04	—	2.6127e-10	—	8.5024e-06	—	9.8152e-06	—
11	1.9553e-04	1.9559e-04	2.6127e-10	9.2250e-06	8.5024e-06	2.6115e-05	9.8152e-06	2.3448e-05
12	1.9553e-04	1.9559e-04	2.6127e-10	9.2250e-06	8.5024e-06	2.6115e-05	9.8152e-06	2.3448e-05

Table 7: *Example 2.* Errors errors and majorants w.r.t. the iteration steps for $h = \frac{1}{64}$ and $I = 12$ (both values are measured relative to the increment in $\|p\|_p^2$ and $\|\mathbf{u}\|_u^2$ on the N th time step).

We fix Poisson ratio to be $\nu = 0.2$ and Young modulus $E = 0.594$, which yields the Lamé parameters $\mu = 0.2475$ and $\lambda = 0.1238$. We set $\alpha = 1$ and $\beta = \frac{1}{M} + c_f \phi_0 = 0.1165$, where $M = 1.65 \cdot 10^{10}$, $K_u = K + \frac{\alpha^2}{c_0} = 10.2887$, $c_f = \frac{1}{c_0} \lambda_{\mathbb{K}} \frac{K+4/3\mu}{K_u+4/3\mu} = 0.5827$ $C_F = \frac{1}{\sqrt{2}\pi}$, and $\mathbb{K} = I$, where I is a unit tensor. From parameters above, it follows that $L = \frac{\alpha^2}{2(\lambda+2\mu/d)} = 1.3468$ and $q = \frac{L}{\beta+L} = 0.9203$. With such q the ratio $\frac{q^2}{(1-q)^2}$ is 133.3343, which might influence the quantitative quality of the majorant.

We consider 10 time-steps of the length $\tau = 1.0$ discretizing considered interval and spatial mesh-size $h = \frac{1}{64}$ using standard P_1 finite elements (see (6.7)). The number of iterations to solve the problem on each time-step is set to 12. For the time-interval $[t_9, t_{10}] = [9.0, 10.0]$, the convergence of the errors in \mathbf{u} and p is presented by Table 7. From one side, we can consider iterations I and $I - 1$ as subsequent ones with a contraction parameter $q = 0.9203$. However, by using Lemma 2 instead, let $m = 6$ so that 6th and 12th iterations be treated as two consecutive steps but with $q' = q^6 = 0.6027$. Then, the constants dependent from the ratio $\frac{q^2}{(1-q^2)} = 2.3012$ attain more acceptable values. Table 8 illustrates the improvement of error majorants efficiency indices as the explained-above method is employed. The local distribution of the error in p and \mathbf{u} on each cell of the finite-element discretization is presented for mesh sizes $h = 1/4$ and $h = 1/8$ in Figure 2. One can see the resemblance in the local error distribution for p since the exact solutions for both examples are the same. The local values of error and indicator (generated by the majorant) in \mathbf{u} has more uniform distribution.

Realistic parameters. Let us consider more realistic parameters similar to those considered in [71]. Again, let exact pressure be $p(x, y, t) = 10^8 x(1-x)y(1-y)t$. Mechanical parameters such as Biot and bulk modulus are chosen as follows: $M = 1.4514 \cdot 10^4$ [Pa] and $E = 7 \cdot 10^7$ [Pa], respectively. The permeability tensor is $\mathbb{K} = \text{diag}\{50, 200\} \cdot 10^{-10}$ [mD/cP], whereas the fluid viscosity is $\mu_f = 10^{-3}$. Thus, we obtain $\beta = \frac{1}{M} + c_f \phi_0 = 6.8909 \cdot 10^{-5}$, which, in turn, yields considerable small $L = \frac{\alpha^2}{2(\lambda+2\mu/d)} = 1.1428 \cdot 10^{-8}$. Such parameter generates contractive parameter $q = \frac{L}{\beta+L} = 1.6584 \cdot 10^{-4}$. The latter means that the ratio $\frac{q^2}{(1-q)^2}$ is of order 10^{-8} , which does not degenerate the efficiency of the majorant. We summarise the convergence results in Table 9. It confirms that even for more realistic parameters (common for engineering applications), the value of the estimates remains rather efficient.

Conclusion

We analyze semi-discrete approximations of the Biot poroelastic problem and deduce guaranteed and fully computable bounds of corresponding errors. The derivation combines estimates for contraction mappings and functional a posteriori error majorants for the elliptic problems. An extended version of the paper that contains an overview of the related works and derivation of the model as well as detailed proofs can be found in [62].

h	$\ e_p\ ^2$	$\ e_u\ ^2$	$[(e_u, e_p)]$	$I_{\text{eff}}(\bar{M}_p)$	$I_{\text{eff}}(\bar{M}_u)$	$I_{\text{eff}}(\bar{M})$
(a) $N = 10, \quad \tau = 1.0$						
$1/4$	5.0147e-02	2.1767e-03	2.5823e-03	40.48 → 4.94	20.61 → 3.15	24.81 → 3.49
$1/8$	1.2525e-02	5.4416e-04	6.4546e-04	40.46 → 4.93	20.59 → 3.15	24.78 → 3.49
$1/16$	3.1293e-03	1.3604e-04	1.6135e-04	40.46 → 4.93	20.58 → 3.15	24.78 → 3.49
$1/32$	7.8217e-04	3.4010e-05	4.0335e-05	40.46 → 4.93	20.58 → 3.15	24.77 → 3.49
$1/64$	1.9553e-04	8.5024e-06	1.0084e-05	40.46 → 4.93	20.58 → 3.15	24.77 → 3.49
(b) $N = 10^2, \quad \tau = 0.1$						
$1/4$	4.7811e-02	4.7811e-02	2.5836e-04	129.34 → 15.18	20.34 → 3.12	54.62 → 6.67
$1/8$	1.1914e-02	5.4416e-05	6.4554e-05	129.53 → 15.27	20.33 → 3.12	54.62 → 6.70
$1/16$	2.9748e-03	1.3604e-05	1.6135e-05	129.60 → 15.27	20.33 → 3.14	54.62 → 6.81
$1/32$	7.4345e-04	3.4010e-06	4.0336e-06	129.62 → 16.66	20.33 → 3.23	54.62 → 7.21
$1/64$	1.8585e-04	8.5024e-07	1.0084e-06	129.62 → 20.45	20.33 → 3.56	54.62 → 8.74

Table 8: *Example 2*. Convergence of errors and majorants w.r.t. the different choice of spatial mesh sizes and time steps (measured relatively w.r.t. $\|p_h^i\|_p^2$ and $\|u_h^i\|_u^2$).

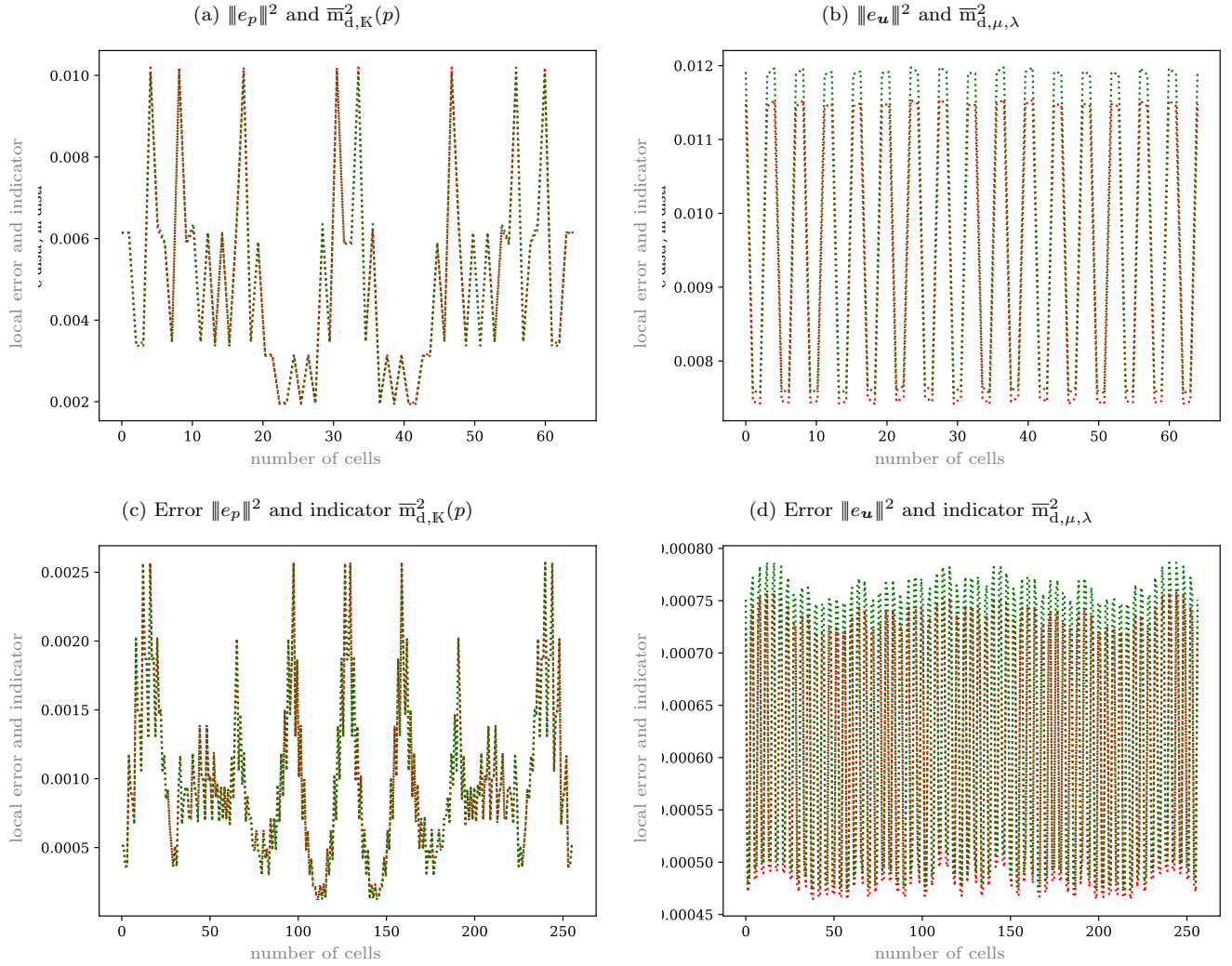


Figure 2: *Example 2*. Errors $\|e_p\|^2$ and $\|e_u\|^2$ (in red) and error indicators $\bar{m}_{d,K}^2$ and $\bar{m}_{d,\mu,\lambda}^2$ (in green) generated by the majorants \bar{M}_p^h and \bar{M}_u^h , respectively, distributions w.r.t. to the numbered finite element cells.

h	$\ e_p\ ^2$	\bar{M}_p	$\ e_u\ ^2$	\bar{M}_u	$[(e_u, e_p)]^2$	\bar{M}	$I_{\text{eff}}(\bar{M})$
(a) $N = 10$, $\tau = 1.0$							
$1/4$	3.9463e-02	2.0213e-01	2.1767e-03	1.3970e-02	3.9663e-02	2.0342e-01	2.26
$1/8$	9.6879e-03	4.9714e-02	5.4416e-04	3.4872e-03	9.7380e-03	5.0034e-02	2.27
$1/16$	2.4097e-03	1.2333e-02	1.3604e-04	8.7104e-04	2.4222e-03	1.2413e-02	2.26
$1/32$	6.0164e-04	3.0727e-03	3.4010e-05	2.1767e-04	6.0477e-04	3.0927e-03	2.26
$1/64$	1.5036e-04	7.6693e-04	8.5024e-06	5.4407e-05	1.5114e-04	7.7193e-04	2.26
(a) $N = 100$, $\tau = 0.1$							
$1/4$	1.5307e-02	5.5755e-02	2.1767e-04	1.2482e-03	1.5375e-02	5.6145e-02	1.91
$1/8$	3.4085e-03	1.3741e-02	5.4416e-05	3.1213e-04	3.4255e-03	1.3839e-02	2.01
$1/16$	8.2572e-04	3.4190e-03	1.3604e-05	7.8032e-05	8.2996e-04	3.4433e-03	2.04
$1/32$	2.0478e-04	8.5343e-04	3.4010e-06	1.9508e-05	2.0584e-04	8.5952e-04	2.04
$1/64$	5.1091e-05	2.1324e-04	8.5024e-07	4.8769e-06	5.1356e-05	2.1477e-04	2.04
(a) $N = 10^3$, $\tau = 0.01$							
$1/4$	4.5193e-03	7.0435e-03	2.1767e-05	1.2204e-04	4.5282e-03	7.0936e-03	1.25
$1/8$	6.0419e-04	1.7367e-03	5.4416e-06	3.0530e-05	6.0642e-04	1.7493e-03	1.70
$1/16$	1.1831e-04	4.3238e-04	1.3604e-06	7.6332e-06	1.1887e-04	4.3552e-04	1.91
$1/32$	2.7537e-05	1.0798e-04	3.4010e-07	1.9084e-06	2.7677e-05	1.0876e-04	1.98

Table 9: *Example 2.* Convergence of errors and majorants w.r.t. the different choice of spatial mesh sizes and time steps (measured relatively w.r.t. $\|p_h^i\|_p^2$ and $\|u_h^i\|_u^2$).

Acknowledgment

The work is funded by the SIU Grant CPRU-2015/10040. The second author wants to acknowledge the support of the Austrian Science Fund (FWF), in particular, the NFN S117-03 project. KK and JMN would like to acknowledge Norwegian Research Council project Toppforsk 250223 for funding.

References

- [1] K. Terzaghi, Principle of soil mechanics, Eng. News Record, A Series of Articles, 1925.
- [2] M. Biot, General theory of three-dimensional consolidation, Journal of applied physics 12 (1941) 155–164.
- [3] M. Biot, Theory of elasticity and consolidation for a porous anisotropic solid, Journal of applied physics 26 (195) 182–185.
- [4] O. Coussy, Mechanics of porous continua, Wiley, West Sussex, 1995.
- [5] R. E. Showalter, Diffusion in poro-elastic media, J. Math. Anal. Appl. 251 (2000) 310–340.
- [6] R. E. Showalter, U. Stefanelli, Diffusion in poro-plastic media, Math. Methods Appl. Sci. 27 (2004) 2131–2151.
- [7] M. A. Murad, A. F. D. Loula, Improved accuracy in finite element analysis of Biot’s consolidation problem, Comput. Methods Appl. Mech. Engrg. 95 (1992) 359–382.
- [8] A. Mikelić, M. F. Wheeler, Theory of the dynamic Biot-Allard equations and their link to the quasi-static Biot system, J. Math. Phys. 53 (2012) 123702, 15.
- [9] A. Settari, F. Mourits, A coupled reservoir and geomechanical simulation system, SPE J. 3 (1998) 219–226.
- [10] T. Almani, K. Kumar, M. F. Wheeler, Convergence and error analysis of fully discrete iterative coupling schemes for coupling flow with geomechanics, Comput. Geosci. 21 (2017) 1157–1172.
- [11] K. Kumar, T. Almani, G. Singh, M. F. Wheeler, Multirate undrained splitting for coupled flow and geomechanics in porous media, in: Numerical mathematics and advanced applications—ENUMATH 2015, volume 112 of *Lect. Notes Comput. Sci. Eng.*, Springer, [Cham], 2016, pp. 431–440.

- [12] T. Almani, K. Kumar, A. Dogru, G. Singh, M. F. Wheeler, Convergence analysis of multirate fixed-stress split iterative schemes for coupling flow with geomechanics, *Comput. Methods Appl. Mech. Engrg.* 311 (2016) 180–207.
- [13] P. A. Vermeer, A. Verruijt, An accuracy condition for consolidation by finite elements, *Internat. J. Numer. Analyt. Methods Geomech.* 5 (1981) 1–14.
- [14] M. B. Reed, An investigation of numerical errors in the analysis of consolidation by finite elements, *Internat. J. Numer. Anal. Methods Geomech.* 8 (1984) 243–257.
- [15] O. C. Zienkiewicz, T. Shiomi, Dynamic behaviour of saturated porous media; the generalized Biot formulation and its numerical solution, *Internat. J. Numer. Anal. Methods Geomech.* 8 (1984) 71–96.
- [16] M. A. Murad, A. F. D. Loula, On stability and convergence of finite element approximations of Biot’s consolidation problem, *Internat. J. Numer. Methods Engrg.* 37 (1994) 645–667.
- [17] M. A. Murad, V. Thomée, A. F. D. Loula, Asymptotic behavior of semidiscrete finite-element approximations of Biot’s consolidation problem, *SIAM J. Numer. Anal.* 33 (1996) 1065–1083.
- [18] J. Korsawe, G. Starke, A least-squares mixed finite element method for Biot’s consolidation problem in porous media, *SIAM J. Numer. Anal.* 43 (2005) 318–339.
- [19] J. M. Nordbotten, Stable cell-centered finite volume discretization for Biot equations, *SIAM J. Numer. Anal.* 54 (2016) 942–968.
- [20] Y. Chen, Y. Luo, M. Feng, Analysis of a discontinuous Galerkin method for the Biot’s consolidation problem, *Appl. Math. Comput.* 219 (2013) 9043–9056.
- [21] D. Boffi, M. Botti, D. A. Di Pietro, A nonconforming high-order method for the Biot problem on general meshes, *SIAM J. Sci. Comput.* 38 (2016) A1508–A1537.
- [22] J. Vignollet, S. May, R. de Borst, On the numerical integration of isogeometric interface elements, *Internat. J. Numer. Methods Engrg.* 102 (2015) 1733–1749.
- [23] S.-H. Chan, K.-K. Phoon, F. H. Lee, A modified jacobi preconditioner for solving ill-conditioned Biots consolidation equations using symmetric quasi-minimal residual method, *Internat. J. Numer. Anal. Methods Geomech.* 25 (2001) 1001–1025.
- [24] K. K. Phoon, K. C. Toh, S. H. Chan, F. H. Lee, An efficient diagonal preconditioner for finite element solution of Biot consolidation equations, *J. Numer. Methods Engrg.* 55 (2002) 377–400.
- [25] J. A. White, R. I. Borja, Block-preconditioned Newton-Krylov solvers for fully coupled flow and geomechanics, *Comput. Geosci.* 15 (2011) 647–659.
- [26] J. B. Haga, H. Osnes, H. P. Langtangen, A parallel block preconditioner for large-scale poroelasticity with highly heterogeneous material parameters, *Comput. Geosci.* 16 (2012) 723–734.
- [27] O. Axelsson, R. Blaheta, P. Byczanski, Stable discretization of poroelasticity problems and efficient preconditioners for arising saddle point type matrices, *Comput. Vis. Sci.* 15 (2012) 191–207.
- [28] J. B. Haga, H. Osnes, H. P. Langtangen, A parallel block preconditioner for large-scale poroelasticity with highly heterogeneous material parameters, *Comput. Geosci.* 16 (2012) 723–734.
- [29] N. Castelletto, J. White, H. Tchelepi, Accuracy and convergence properties of the fixed-stress iterative solution of two-way coupled poromechanics, *Int. J. Numer. Anal. Methods Geomech.* 39 (2015) 1593–1618.
- [30] N. Castelletto, J. White, M. Ferronato, Scalable algorithms for three-field mixed finite element coupled poromechanics, *J. Comput. Phys.* 327 (2016) 894–918.
- [31] S. Rhebergen, G. N. Wells, R. F. Katz, A. J. Wathen, Analysis of block preconditioners for models of coupled magma/mantle dynamics, *SIAM J. Sci. Comput.* 36 (2014) A1960–A1977.

- [32] S. Rhebergen, G. N. Wells, A. J. Wathen, R. F. Katz, Three-field block preconditioners for models of coupled magma/mantle dynamics, *SIAM J. Sci. Comput.* 37 (2015) A2270–A2294.
- [33] Q. Hong, J. Kraus, Uniformly stable discontinuous Galerkin discretization and robust iterative solution methods for the Brinkman problem, *SIAM J. Numer. Anal.* 54 (2016) 2750–2774.
- [34] J. J. Lee, K.-A. Mardal, R. Winther, Parameter-robust discretization and preconditioning of Biot’s consolidation model, *SIAM J. Sci. Comput.* 39 (2017) A1–A24.
- [35] T. Bæ rland, J. J. Lee, K.-A. Mardal, R. Winther, Weakly imposed symmetry and robust preconditioners for Biot’s consolidation model, *Comput. Methods Appl. Math.* 17 (2017) 377–396.
- [36] D. Allen, Stability, accuracy, and efficiency of sequential methods for coupled flow and geomechanics, Technical Report SPE119084, The SPE Reservoir Simulation Symposium, Houston, Texas, 2009.
- [37] J. A. White, N. Castelletto, H. A. Tchelepi, Block-partitioned solvers for coupled poromechanics: a unified framework, *Comput. Methods Appl. Mech. Engrg.* 303 (2016) 55–74.
- [38] F. J. Gaspar, C. Rodrigo, On the fixed-stress split scheme as smoother in multigrid methods for coupling flow and geomechanics, *Comput. Methods Appl. Mech. Engrg.* 326 (2017) 526–540.
- [39] Q. Hong, K. J. , Parameter-robust stability of classical three-field formulation of Biot consolidation model, arXiv.org arXiv:1706.00724v2 [math.NA] (2017).
- [40] S. Meunier, Analyse derreur a posteriori pour les couplages hydro-Mcaniques et mise en oeuvre dans, Ph.D. thesis, cole des Ponts ParisTech, 2007.
- [41] A. Ern, S. Meunier, A posteriori error analysis of Euler-Galerkin approximations to coupled elliptic-parabolic problems, *M2AN Math. Model. Numer. Anal.* 43 (2009) 353–375.
- [42] M. Vohralík, M. F. Wheeler, A posteriori error estimates, stopping criteria, and adaptivity for two-phase flows, *Comput. Geosci.* 17 (2013) 789–812.
- [43] S. Yousef, A posteriori error estimates and adaptivity based on stopping criteria and adaptive mesh re finement for multiphase and thermal flows. Application to steam-assisted gravity drainage, Ph.D. thesis, Universit Pierre et Marie Curie - Paris VI, 2013.
- [44] D. A. Di Pietro, M. Vohralík, S. Yousef, An a posteriori-based, fully adaptive algorithm with adaptive stopping criteria and mesh refinement for thermal multiphase compositional flows in porous media, *Comput. Math. Appl.* 68 (2014) 2331–2347.
- [45] D. A. Di Pietro, E. Flauraud, M. Vohralík, S. Yousef, A posteriori error estimates, stopping criteria, and adaptivity for multiphase compositional Darcy flows in porous media, *J. Comput. Phys.* 276 (2014) 163–187.
- [46] E. Ahmed, S. A. Hassan, C. Japhet, M. Kern, M. Vohralík, A posteriori error estimates and stopping criteria for space-time domain decomposition for two-phase flow between different rock types, Technical Report hal-01540956, version 1, HAL, 2017.
- [47] F. Larsson, K. Runesson, A sequential-adaptive strategy in space-time with application to consolidation of porous media, *Comput. Methods Appl. Mech. Engrg.* 288 (2015) 146–171.
- [48] R. Riedlbeck, D. A. Di Pietro, A. Ern, S. Granet, K. Kazymyrenko, Stress and flux reconstruction in Biot’s poro-elasticity problem with application to a posteriori error analysis, *Comput. Math. Appl.* 73 (2017) 1593–1610.
- [49] F. Bertrand, M. Moldenhauer, G. Starke, A posteriori error estimation for planar linear elasticity by stress reconstruction, Technical Report arXiv:1703.00436, arXiv, 2017.
- [50] E. Ahmed, F. A. Radu, J. M. Nordbotten, Adaptive poromechanics computations based on a posteriori error estimates for fully mixed formulations of Biot’s consolidation model, *Comput. Methods Appl. Mech. Engrg.* 347 (2019) 264–294.

- [51] E. Ahmed, J. M. Nordbotten, F. A. Radu, Adaptive asynchronous time-stepping, stopping criteria, and a posteriori error estimates for fixed-stress iterative schemes for coupled poromechanics problems, *J. Comput. Appl. Math.* 364 (2020).
- [52] J. M. Nordbotten, T. Rahman, S. I. Repin, J. Valdman, A posteriori error estimates for approximate solutions of the Barenblatt-Biot poroelastic model, *Comput. Methods Appl. Math.* 10 (2010) 302–314.
- [53] S. Banach, Sur les opérations dans les ensembles abstraits et leur application aux équations intégrales, *Fund. Math.* 3 (1922) 133–181.
- [54] S. Repin, A posteriori estimates for partial differential equations, volume 4 of *Radon Series on Computational and Applied Mathematics*, Walter de Gruyter GmbH & Co. KG, Berlin, 2008.
- [55] O. Mali, P. Neittaanmäki, S. Repin, Accuracy verification methods, volume 32 of *Computational Methods in Applied Sciences*, Springer, Dordrecht, 2014. Theory and algorithms.
- [56] A. Ženišek, The existence and uniqueness theorem in Biot’s consolidation theory, *Apl. Mat.* 29 (1984) 194–211.
- [57] R. E. Showalter, N. Su, Partially saturated flow in a poroelastic medium, *Discrete Contin. Dyn. Syst. Ser. B* 1 (2001) 403–420.
- [58] A. Mikelić, M. F. Wheeler, Convergence of iterative coupling for coupled flow and geomechanics, *Comput. Geosci.* 17 (2013) 455–461.
- [59] A. Mikelić, B. Wang, M. F. Wheeler, Numerical convergence study of iterative coupling for coupled flow and geomechanics, *Comput. Geosci.* 18 (2014) 325–341.
- [60] J. Kim, H. A. Tchelepi, R. Juanes, Stability and convergence of sequential methods for coupled flow and geomechanics: drained and undrained splits, *Comput. Methods Appl. Mech. Engrg.* 200 (2011) 2094–2116.
- [61] J. Kim, H. A. Tchelepi, R. Juanes, Stability and convergence of sequential methods for coupled flow and geomechanics: fixed-stress and fixed-strain splits, *Comput. Methods Appl. Mech. Engrg.* 200 (2011) 1591–1606.
- [62] K. Kumar, S. Matculevich, J. Nordbotten, S. Repin, Guaranteed and computable bounds of approximation errors for the semi-discrete Biot problem, Technical Report [math.NA]:1808.08036, arXiv, 2018.
- [63] S. Repin, A posteriori estimates for approximate solutions of variational problems with strongly convex functionals, *Problems of Mathematical Analysis* 17 (1997) 199–226.
- [64] S. Repin, A posteriori error estimation for variational problems with uniformly convex functionals, *Math. Comput.* 69 (2000) 481–500.
- [65] P. Neittaanmäki, S. Repin, Reliable methods for computer simulation, volume 33 of *Studies in Mathematics and its Applications*, Elsevier Science B.V., Amsterdam, 2004. Error control and a posteriori estimates.
- [66] J. W. Both, M. Borregales, J. M. Nordbotten, K. Kumar, F. A. Radu, Robust fixed stress splitting for Biot’s equations in heterogeneous media, *Applied Mathematics Letters* 68 (2017) 101–108.
- [67] J. W. Both, U. Koecher, Numerical investigation on the fixed-stress splitting scheme for Biots equations: Optimality of the tuning parameter, arXiv.org arXiv:1801.08352 [math.NA] (2018).
- [68] S. Repin, S. Sauter, Functional a posteriori estimates for the reaction-diffusion problem, *C. R. Acad. Sci. Paris* 343 (2006) 349–354.
- [69] D. N. Arnold, F. Brezzi, Mixed and nonconforming finite element methods: implementation, postprocessing and error estimates, *RAIRO Modél. Math. Anal. Numér.* 19 (1985) 7–32.
- [70] D. N. Arnold, Mixed finite element methods for elliptic problems, *Comput. Methods Appl. Mech. Engrg.* 82 (1990) 281–300. Reliability in computational mechanics (Austin, TX, 1989).

- [71] V. Girault, M. F. Wheeler, B. Ganis, M. E. Mear, A lubrication fracture model in a poro-elastic medium, *Math. Models Methods Appl. Sci.* 25 (2015) 587–645.
- [72] O. A. Ladyzhenskaya, *The boundary value problems of mathematical physics*, Springer, New York, 1985.
- [73] O. A. Ladyzhenskaya, V. A. Solonnikov, N. Uraltseva, *Linear and quasilinear equations of parabolic type*, Nauka, Moscow, 1967.
- [74] E. Zeidler, *Nonlinear functional analysis and its applications. II/A*, Springer-Verlag, New York, 1990. *Linear monotone operators*, Translated from the German by the author and Leo F. Boron.

Appendix

Notation and definitions of spaces. We use standard Lebesgue space of square-measurable functions $L^2(\Omega)$ equipped with the norm $\|v\|_\Omega := \|v\|_{L^2(\Omega)} := (v, v)_\Omega^{1/2}$ for all $u, v \in L^2(\Omega)$. Let $\mathbf{M}^{d \times d}$ denote the space of real d -dimensional tensors. Product for vector-valued functions $\mathbf{v}, \mathbf{w} \in \mathbb{R}^d$ and tensor-valued functions $\boldsymbol{\tau}, \boldsymbol{\sigma} \in \mathbf{M}^{d \times d}$ are defined by the relations

$$(\mathbf{v}, \mathbf{w})_\Omega := \int_\Omega \mathbf{v} \cdot \mathbf{w} \, dx \quad \text{and} \quad (\boldsymbol{\tau}, \boldsymbol{\sigma})_\Omega := \int_\Omega \boldsymbol{\tau} : \boldsymbol{\sigma} \, dx,$$

where $\mathbf{v} \cdot \mathbf{w} := v_i w_i$ and $\boldsymbol{\tau} : \boldsymbol{\sigma} := \tau_{ij} \sigma_{ij}$, respectively. Next, $\mathbf{A}(x) \in \mathbf{M}^{d \times d}$, $x \in \Omega$ denotes a symmetric uniformly positive defined matrix that satisfies $0 < \underline{\lambda} \leq \lambda(x) \leq \bar{\lambda} \leq +\infty$, $\underline{\lambda}, \bar{\lambda} \in \mathbb{R}$, with uniformly bounded eigenvalues $\lambda(x)$. Then, for the product $(\mathbf{u}, \mathbf{v})_{\mathbf{A}} := (\mathbf{A}\mathbf{u}, \mathbf{v})$, we have

$$\underline{\lambda} \|\mathbf{v}\| \leq \|\mathbf{v}\|_{\mathbf{A}} \leq \bar{\lambda} \|\mathbf{v}\| \quad \text{and} \quad (\mathbf{u}, \mathbf{v}) \leq \|\cdot\|_{\mathbf{A}} \|\cdot\|_{\mathbf{A}^{-1}}, \quad \forall \mathbf{u}, \mathbf{v} \in [L^2(\Omega)]^d.$$

We use the standard notation for the Sobolev space of vector-valued functions having square-summable derivatives

$$H^1(\Omega) := \{v \in L^2(\Omega) \mid \nabla v \in [L^2(\Omega)]^d\},$$

equipped with the norm $\|v\|_{H^1(\Omega)} := (\|v\|_\Omega^2 + |\nabla v|_\Omega^2)^{1/2}$. Also, we use the semi-norm $|v|_\Omega := |v|_{H^1(\Omega)} := \|\nabla v\|_\Omega$, and for the the vector-valued functions with square-summable divergence introduce the Hilbert space

$$H(\Omega, \text{div}) := \{\mathbf{v} \in [L^2(\Omega)]^d \mid \text{div} \mathbf{v} \in L^2(\Omega)\},$$

endowed with the norm $\|\mathbf{v}\|_{H(\Omega, \text{div})}^2 := \|\mathbf{v}\|_{[L^2(\Omega)]^d}^2 + \|\text{div} \mathbf{v}\|_{L^2(\Omega)}^2$.

Let Σ be a part of the boundary such that $\text{meas}_{d-1} \Sigma > 0$ (in particular, may coincide with $\partial\Omega$). For functions in $H_{0,\Sigma}^1(\Omega) := \{v \in H^1(\Omega) \mid v|_\Sigma = 0\}$, the Friedrichs'-type inequality reads:

$$\|v\|_\Omega \leq C_\Gamma^{\text{F}} |v|_\Omega, \quad \forall v \in H_{0,\Sigma}^1(\Omega). \quad (6.2)$$

The corresponding trace operator $\gamma : H^1(\Omega) \rightarrow H^{\frac{1}{2}}(\Sigma)$ is bounded and satisfies the estimate

$$v|_\Sigma := \gamma v, \quad \|v|_\Sigma\| \leq C_{\Sigma\Omega}^{\text{tr}} \|v\|_{H^1(\Omega)}, \quad \forall v \in H^1(\Omega), \quad (6.3)$$

where $\|v|_\Sigma\|$ is the norm of $L^2(\Sigma)$.

C_K denotes the constant in the Korn inequality

$$\|\mathbf{w}\|_{[H^1(\Omega)]^d} \leq C_K \|\boldsymbol{\varepsilon}(\mathbf{w})\|_{[L^2(\Omega)]^{d \times d}}, \quad \forall \mathbf{w} \in [H^1(\Omega)]^d, \quad (6.4)$$

Also, we use the inequality

$$\|\text{div} \mathbf{w}\| = \|\text{tr} \boldsymbol{\varepsilon}(\mathbf{w})\| = \|\mathbf{I} : \boldsymbol{\varepsilon}(\mathbf{w})\| \leq \sqrt{d} \|\boldsymbol{\varepsilon}(\mathbf{w})\|, \quad \forall \mathbf{w} \in [H^1(\Omega)]^d, \quad (6.5)$$

where $\mathbf{I} \in \mathbf{M}^{d \times d}$ is the unit tensor of $\mathbf{M}^{d \times d}$, and $\boldsymbol{\varepsilon}(\mathbf{w}) \in \mathbf{M}^{d \times d}$ denotes the symmetric part of $\nabla \mathbf{w}$.

Next, let $Q := \Omega \times (0, T)$ denote a space-time cylinder (with given time-interval $(0, T)$, $0 < T < +\infty$), and let $\Sigma = \partial\Omega \times (0, T)$ be a lateral surface of Q , whereas $\Sigma_0 := \partial\Omega \times \{0\}$ and $\Sigma_T := \partial\Omega \times \{T\}$ define the bottom and the top parts of the mantle (so that $\partial Q = \Sigma \cup \Sigma_0 \cup \Sigma_T$). Consider functions defined in $(0, T)$ with values in a functional space X (cf. [72, 73, 74]). Let $\|\cdot\|_X$ denote the norm in X , then for $r = 2$, we define the Bochner space

$$L^2(0, T; X) := \left\{ f \text{ measurable in } [0, T] \mid \int_0^T \|f(t)\|_X^2 dt < \infty \right\},$$

and respective norm $\|f\|_{L^2(0, T; X)} := \left(\int_0^T \|f(t)\|_X^2 dt \right)^{1/2}$. It is a Hilbert space if X is a Hilbert space. Throughout the paper, we also use the spaces

$$H^1(0, T; X) := \{ f \in L^2(0, T; X) \mid \partial_t f \in L^2(0, T; X) \} \quad (6.6)$$

equipped with norm $\|u\|_{H^1(0, T; X)} := \left(\int_0^T (\|\partial_t f(t)\|_X^2 + \|f(t)\|_X^2) dt \right)^{1/2}$.

We assume that \mathcal{T}_h is a regular mesh satisfying angle condition defined on Ω . Then, the corresponding discretization spaces with the Lagrangian finite elements of order 0 or 1 are defined as

$$\mathbb{P}_0 := \{v_h \in L^2(\Omega) \mid \forall T \in \mathcal{T}_h, v_h|_T \in \mathbb{P}_0\}, \quad \mathbb{P}_1 := \{v_h \in H^1(\Omega) \mid \forall T \in \mathcal{T}_h, v_h|_T \in \mathbb{P}_1\}, \quad (6.7)$$

where \mathbb{P}_k denotes the space of polynomials of the order $k \in \mathbb{N} \cup 0$. The Raviart-thomas elements of the lowest and first order are denoted by

$$\begin{aligned} \mathbb{RT}_0 &:= \{ \mathbf{y}_h \in H(\text{div}, \Omega) : \forall T \in \mathcal{T}_h, \mathbf{y}_h|_T = \mathbf{a} + b \mathbf{x}, \mathbf{a} \in \mathbb{R}^d, b \in \mathbb{R} \}, \\ \mathbb{RT}_1 &:= \{ \mathbf{y}_h \in H(\text{div}, \Omega) : \forall T \in \mathcal{T}_h, \mathbf{y}_h(\mathbf{x})|_T = \mathbf{q}(\mathbf{x}) + \mathbf{x} r(\mathbf{x}), \mathbf{q} \in [\mathbb{P}_1]^d, r \in \mathbb{P}_1 \}, \end{aligned}$$

respectively. Finally, the table below presents notation used on the paper for the physical quantities.

σ_{por}	poroelastic Cauchy stress (total stress) tensor
\mathbf{u}	displacement of the solid
p	fluid pressure
$\boldsymbol{\sigma}$	linear elastic (effective) stress tensor
$\boldsymbol{\varepsilon}(\mathbf{u})$	strain tensor
λ, μ	Lamé paramteres
\mathbf{f}	volumetric body force
\mathbf{w}	Darcy velocity
μ_f	fluid viscosity
\mathbb{K}	permeability tensor
g	gravitation constant
ρ_f	fluid phase density
α	Biot-Willis coefficient
$\beta = \frac{1}{M} + c_f \varphi_0$	storage coefficient
M	Biot constant
c_f	fluid compressibility
φ_0	initial porosity

Table 10: Table of notation

Contraction theorem. An essential part of our analysis is based on the contraction theorem, which was proven in [58] for the poroelastic problem in question. However, Lemma 3 uses the contraction of the sequence $\{\delta(\eta - \eta_h)\}^i$, $\forall \eta \in W_h$, which is proven below.

Theorem 4. *With $\gamma = \frac{\alpha}{\sqrt{\lambda}}$ and $L = \frac{\alpha^2}{2\lambda}$, the sequence $\{\delta(\eta - \eta_h)\}^i \in W_h$, where $\eta^i \in W$ is generated by the fixed-stress split iterative scheme defined in (3.4)–(3.5) and $\eta_h^i \in W_h$ is discretization of the latter sequence, is a contraction given by*

$$\|\boldsymbol{\varepsilon}(\delta(\mathbf{u} - \mathbf{u}_h)^i)\|_{2\mu}^2 + q \|\nabla \delta(p - p_h)^i\|_{\mathbb{K}_\tau}^2 + \|\delta(\eta - \eta_h)^i\|^2 \leq q^2 \|\delta(\eta - \eta_h)^{i-1}\|^2, \quad q = \frac{L}{\beta + L}. \quad (6.8)$$

Proof: Consider the difference between $(i-1)$ th and i th iterations in (3.4) and (3.5). Assuming that $\delta p^i = p^i - p^{i-1}$ and $\delta \mathbf{u}^i = \mathbf{u}^i - \mathbf{u}^{i-1}$, as well as particular chosen $w = w_h \in W_{0h} \subset W_0$ and $\mathbf{v} = \mathbf{v}_h \in \mathbf{V}_{0h} \subset \mathbf{V}_0$ with conforming Galerkin discretization spaces W_{0h} and \mathbf{V}_{0h} of W_0 and \mathbf{V}_0 , respectively. Thus, we obtain

$$(\mathbb{K}_\tau \nabla \delta p^i, \nabla w_h) + (\beta + L)(\delta p^i, w_h) = (-\gamma \delta \eta^{i-1}, w_h), \quad \forall w \in W_{0h}, \quad (6.9)$$

$$(2\mu \boldsymbol{\varepsilon}(\delta \mathbf{u}^i), \boldsymbol{\varepsilon}(\mathbf{v}_h)) + (\lambda \operatorname{div} \delta \mathbf{u}^i, \operatorname{div} \mathbf{v}_h) = (-\alpha \nabla \delta p^i, \mathbf{v}_h), \quad \forall \mathbf{v}_h \in \mathbf{V}_{0h}, \quad (6.10)$$

For Galerkin approximations $(\mathbf{u}, p)_h^i \in \mathbf{V}_{0h} \times W_{0h}$, the system above can be rewritten as

$$(\mathbb{K}_\tau \nabla \delta p_h^i, \nabla w_h) + (\beta + L)(\delta p_h^i, w_h) = (-\gamma \delta \eta_h^{i-1}, w_h), \quad \forall w_h \in W_{0h}, \quad (6.11)$$

$$(2\mu \boldsymbol{\varepsilon}(\delta \mathbf{u}_h^i), \boldsymbol{\varepsilon}(\mathbf{v}_h)) + (\lambda \operatorname{div} \delta \mathbf{u}_h^i, \operatorname{div} \mathbf{v}_h) = (-\alpha \nabla \delta p_h^i, \mathbf{v}_h), \quad \forall \mathbf{v} \in \mathbf{V}_{0h}. \quad (6.12)$$

Difference of (6.9)–(6.10) and (6.11)–(6.12), substitution of $w_h = \delta(p - p_h)^i$ in flow part and $\mathbf{v}_h = \delta(\mathbf{u} - \mathbf{u}_h)^i$ in the corresponding mechanics part yield

$$\|\nabla \delta(p - p_h)^i\|_{\mathbb{K}_\tau}^2 + (\beta + L) \|\delta(p - p_h)^i\|^2 = -\gamma (\delta(\eta - \eta_h)^{i-1}, \delta(p - p_h)^i), \quad \forall w_h \in W_{0h}, \quad (6.13)$$

$$\|\boldsymbol{\varepsilon}(\delta(\mathbf{u} - \mathbf{u}_h)^i)\|_{2\mu}^2 + \|\operatorname{div} \delta(\mathbf{u} - \mathbf{u}_h)^i\|_\lambda^2 = -\alpha (\delta(p - p_h)^i, \operatorname{div} \delta(\mathbf{u} - \mathbf{u}_h)^i), \quad \forall \mathbf{v} \in \mathbf{V}_{0h}. \quad (6.14)$$

Application of the Young inequality in (6.13) provide the relation

$$(\beta + L) \|\delta(p - p_h)^i\|^2 + \|\nabla \delta(p - p_h)^i\|_{\mathbb{K}_\tau}^2 \leq \frac{\epsilon}{2} \|\delta(p - p_h)^i\|^2 + \frac{\gamma^2}{2\epsilon} \|\delta(\eta - \eta_h)^{i-1}\|^2, \quad \epsilon > 0. \quad (6.15)$$

Regrouping similar terms in (6.15) implies

$$(\beta + L - \frac{\epsilon}{2}) \|\delta(p - p_h)^i\|^2 + \|\nabla \delta(p - p_h)^i\|_{\mathbb{K}_\tau}^2 \leq \frac{\gamma^2}{2\epsilon} \|\delta(\eta - \eta_h)^{i-1}\|^2.$$

Substitution of the optimal $\epsilon = \beta + L$, obtained from the minimization problem $\min_{\epsilon > 0} (2\epsilon(\beta + L - \frac{\epsilon}{2}))^{-1}$, yields

$$(\beta + L) \|\delta(p - p_h)^i\|^2 + 2 \|\nabla \delta(p - p_h)^i\|_{\mathbb{K}_\tau}^2 \leq \frac{\gamma^2}{\beta + L} \|\delta(\eta - \eta_h)^{i-1}\|^2. \quad (6.16)$$

By summing (6.16), multiplied by free parameter $c_0 > 0$, and (6.14), we arrive at the following inequality

$$\left\{ c_0 (\beta + L) \|\delta(p - p_h)^i\|^2 + \|\operatorname{div} \delta(\mathbf{u} - \mathbf{u}_h)^i\|_\lambda^2 - \alpha (\delta(p - p_h)^i, \operatorname{div} \delta(\mathbf{u} - \mathbf{u}_h)^i) \right\} \\ + \|\boldsymbol{\varepsilon}(\delta(\mathbf{u} - \mathbf{u}_h)^i)\|_{2\mu}^2 + 2c_0 \|\nabla \delta(p - p_h)^i\|_{\mathbb{K}_\tau}^2 \leq c_0 \frac{\gamma^2}{\beta + L} \|\delta(\eta - \eta_h)^{i-1}\|^2. \quad (6.17)$$

Let us determine the values of parameters c_0 , γ , and L such that the terms in the left-hand side of (6.17) are positive and contraction in $\|\delta(\eta - \eta_h)^{i-1}\|^2$ is achieved. It follows from $\delta(\eta - \eta_h)^i = \frac{\alpha}{\gamma} \operatorname{div} \delta(\mathbf{u} - \mathbf{u}_h)^i - \frac{L}{\gamma} \delta(p - p_h)^i$, that

$$\|\delta(\eta - \eta_h)^i\|^2 = \frac{\alpha^2}{\gamma^2} \|\operatorname{div} \delta(\mathbf{u} - \mathbf{u}_h)^i\|^2 + \frac{L^2}{\gamma^2} \|\delta(p - p_h)^i\|^2 - \frac{2\alpha L}{\gamma^2} (\operatorname{div} \delta(\mathbf{u} - \mathbf{u}_h)^i, \delta(p - p_h)^i). \quad (6.18)$$

Comparing (6.18) and (6.17), we arrive at the following condition on the free parameters:

$$\left\{ \begin{array}{l} \frac{\alpha^2}{\gamma^2} \leq \lambda, \\ \frac{L^2}{\gamma^2} \leq c_0 (\beta + L), \\ \frac{2\alpha L}{\gamma^2} = \alpha, \end{array} \right. \quad \text{which yields} \quad \left\{ \begin{array}{l} L \geq \frac{\alpha^2}{2\lambda}, \\ c_0 \geq \frac{L}{2(\beta + L)}, \\ \gamma^2 = 2L. \end{array} \right.$$

Then, the contraction rate $q = c_0 \frac{\gamma^2}{\beta + L}$ is monotone w.r.t. to L and attains its minimum at

$$L = \frac{\alpha^2}{2\lambda} \quad \text{and} \quad c_0 = \frac{L}{2(\beta + L)}.$$

By using condition $\gamma^2 = 2L$, we obtain

$$\|\boldsymbol{\varepsilon}(\delta(\mathbf{u} - \mathbf{u}_h)^i)\|_{2\mu}^2 + q \|\nabla \delta(p - p_h)^i\|_{\mathbb{K}_\tau}^2 + \|\delta(\eta - \eta_h)^i\|^2 \leq q^2 \|\delta(\eta - \eta_h)^{i-1}\|^2 \quad (6.19)$$

with

$$q = \frac{L}{\beta+L} \quad \text{and} \quad L = \frac{\alpha^2}{2\lambda}.$$

□